Accepted Manuscript

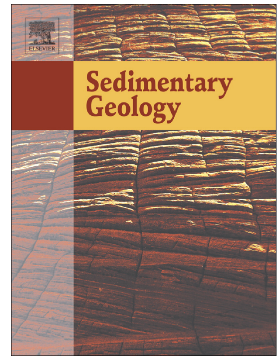

Internal waves as controlling factor in the development of stromatoporoid-rich facies of the Apulia Platform margin (Upper Jurassic-lower cretaceous, Gargano Promontory, Italy)

Farkhondeh Kiani Harchegani, Michele Morsilli

PII: S0037-0738(18)30264-1
DOI: https://doi.org/10.1016/j.sedgeo.2018.11.011
Reference: SEDGEO 5417

To appear in: *Sedimentary Geology*

Received date: 12 September 2018
Revised date: 22 November 2018
Accepted date: 23 November 2018

Please cite this article as: Farkhondeh Kiani Harchegani, Michele Morsilli , Internal waves as controlling factor in the development of stromatoporoid-rich facies of the Apulia Platform margin (Upper Jurassic-lower cretaceous, Gargano Promontory, Italy). Sedgeo (2018), https://doi.org/10.1016/j.sedgeo.2018.11.011

Internal waves as controlling factor in the development of stromatoporoid-rich facies of the Apulia Platform margin (Upper Jurassic-Lower Cretaceous, Gargano Promontory, Italy)

Farkhondeh Kiani Harchegani[a*], Michele Morsilli[a]

[a] Dipartimento di Fisica e Scienze della Terra, Università di Ferrara, Italy

Corresponding author: knhfkh@unife.it

Abstract:

During the Late Jurassic, stromatoporoid-rich buildups were developed in south and intra-Tethys realms. These stromatoporoid buildups are mainly characterized by the high percentage of intraclastic-bioclastic debris, as main components of buildup bodies. However, the source of hydrodynamic energy resulted in debris production, is still a matter of debate. This study examines the Upper Jurassic- Lower Cretaceous stromatoporoid-rich buildups of Monte Sacro Limestones (MSL), Apulia Carbonate Platform (ACP), in order to describe the main carbonate facies along the study area, as well as the possible source of turbulence. Three main lithofacies have been distinguished: LF1- stromatoporoid-rich facies with two subfacies (LF1-S1: floatstone with wackestone to fine-grained packstone, LF1-S2: rudstone-floatstone with intraclastic-bioclastic packstone-grainstone), LF2- stromatoporoid-coral facies distributed in wackestone to packstone matrix (LF2-S2) and tabular stromatoporoid-corals surrounded by wackestone matrix (LF2-S2) and, LF3- stromatoporoid-microbial facies. These facies were deposited along the mid part of a distally steepened ramp. The *in-growth* form of stromatoporoids were developed in a mud-dominated matrix (LF1-S2) under low-energy conditions while the intraclastic-bioclastic rich facies (LF1-S2) were deposited under a high-energy condition. The distribution of LF2 and LF3 in muddy matrix suggests occurrence of these lithofacies in quiet environments.

The biotas were influenced by several factors including nutrient and light availability as well as by hydrodynamism. The stromatoporoid-rich buildups in ACP can be categorized as phototrophic-heterotrophic reefs generated in a pure carbonate environment. The light penetration was confined, resulted in the high development of light-independent micro-encrusters (*Tubiphytes morronensis*), in a mesophotic condition, where the environment was not ideal for light-dependent microencrusters (*Lithocodium- Bacinella*) to grow.
We suggest that debris-rich stromatoporoid-rich lithofacies (LF1) thrived in meso-oligophotic setting, along the nutricline and were affected by more than episodic high-energy events in a context where the surface waves were not effective. In such environments, internal waves can be an effective candidate to explain the episodic turbulences to produce the debris-rich facies of LF1-S2. Moreover, internal waves can pump the nutrient-rich waters to the buildups, and create an ideal setting where these metazoan communities thrived.

Keywords: stromatoporoid, Upper Jurassic reefs, Apulia Carbonate Platform (ACP), internal waves, debris-rich reefs

1. Introduction

The Late Jurassic was a period of extensive reef development, and it represents the peak in diversity of reef- builder organisms (Kiessling, 2002, 2009; Leinfelder et al., 2002; Cecca et al., 2005; Pomar and Hallock, 2008; Martin-Garin et al., 2012; Olivier et al., 2012). During this time the level of CO_2 was at least four times higher than the present and resulted in a high pressure of CO2 ($p$$CO_2$) and therefore a greenhouse condition (Holz, 2015), which favoured the development of abundant microbialite and benthic automicrite factory (Pomar and Hallock, 2008). Global sea-level rose until the end of the Kimmeridgian (Haq, 2018) and this rise was associated with the development of Upper Jurassic reefs domains especially on the European part of the northern Tethys Ocean (Leinfelder et al., 2002).

Upper Jurassic reefs have been studied in details with particular attention on northern part of Tethys and North Atlantic (Dupraz and Strasser, 1999, 2002; Insalaco, 1999; Olivier et al., 2004, 2007; 2012; Lathuilière et al., 2005; Reolid et al., 2007; Strasser and Védrine, 2009; Matyszkiewicz et al., 2012; San Miguel et al., 2017). On the contrary, southern and intra-Tethys reefs received less attention in the literatures (Catalano and D'Argenio, 1981; Turnšek et al., 1981; Morsilli and Bosellini, 1997; Leinfelder et al., 2005; Schlagintweit et al., 2005; Schlagintweit and Gawlick, 2008; Rusciadelli et al., 2011; Basilone and Sulli, 2016a; Hoffmann et al., 2017).

During the Late Jurassic, different types of reefs were developed along the northern and southern part of Tethys (Fig.1). Corals, sponges, and microbialites were the main bioconstructors, particularly in the northern Tethys margin and North Atlantic (Leinfelder et al., 2002), and depositional geometries and facies distribution were mainly ascribed to carbonate ramps (Leinfelder, 1993; Insalaco et al., 1997; Olóriz et al., 2003; San Miguel et al., 2017). Coral reefs widespread in the distal part of the inner ramp of north Tethys, while mid-ramp settings were characterized by mixed coral-siliceous sponge reefs (Leinfelder et al., 2002) as well as coral-microbial reefs in the western part of Tethys (Bádenas and Aurell, 2010). Instead, siliceous sponge mounds thrived in the outer-ramp setting (Dromart et al., 1994; Leinfelder et al., 2002; Olivier et al., 2007; Guo et al., 2011). In contrast, in the southern part of Tethys, including intra-Tethys, the stromatoporoids (inc. chaetetids) were more abundant than corals (Turnšek et al., 1981; Wood, 1999; Leinfelder et al., 2002). These buildups were mostly developed on the margin of isolated platforms (Morsilli and Bosellini, 1997; Rusciadelli et al., 2011) (Fig.1) as well as mid- ramp settings (Al-Awwad and Pomar, 2015).

According to various authors, during the middle to late Oxfordian, in the western and northern Tethys, coral reefs were mainly developed in shallow water settings accompanied with stromatoporoid as a minor constructor (Pandey and Fürsich, 2003; Lathuilière et al., 2005; Guo et al., 2011; Strasser et al., 2015). Microsolenid corals were also formed in the more distal part of the margin (Insalaco et al., 1997; Insalaco, 1999). Siliceous sponges- microbial mounds were widely distributed in the deeper shelf (Guo et al., 2011; Krajewski et al., 2016), while microbialite-rich reefs were expanded in western Tethys and North Atlantic (Reolid et al., 2005) (Fig.1). During the Kimmeridgian coral-microbial reefs flourished (Olivier et al., 2003, 2008; San Miguel et al., 2017) (Fig.1), instead siliceous sponges were developed locally (Leinfelder et al., 1993). In the North Atlantic, sponge reefs, mixed sponge-coral reefs, and bivalve reefs were dominant (Leinfelder et al., 2002). During the Tithonian, scatter coral reefs were distributed compared with Oxfordian to Kimmeridgian time (Leinfelder et al., 2002).

On the other hand, in the southern Tethys and intra- Tethys, the main reefs were made generally by debris-rich stromatoporoid-coral, without main variation from the Oxfordian to the Tithonian (Leinfelder et al., 2002) (Fig.1). In the southern Tethys, different type of stromatoporoids associated with corals have been developed along the shallow shelf of the Arabian plate and the Zagros Basin during the Kimmeridgian and Tithonian (Kano et al., 2007; Al-Awwad and Pomar, 2015; El- Sabbagh et al., 2017) (Fig.1).

Reef growth is controlled by several factors, including light penetration, energy level, sedimentation rate, substrate, nutrient, and salinity, among others (e.g. Hallock, 2015), and their complex interaction. The concept of the tropical carbonate factory is associated with the carbonate production that occurs in oligotrophic, warm and well- illuminated waters of the tropics and subtropics (Schlager, 2000, 2003; Hallock, 2005). In this condition, the light penetration is one of the fundamental factor controlling loci, amount and type of carbonate production, and can be used as a useful tool to reconstruct different zone in the rock record (Bosscher and Schlager, 1992; Pomar, 2001; Wilson and Vecsei, 2005; Morsilli et al., 2012; Pomar et al., 2015; Michel et al., 2018). These zones are named “euphotic”, “oligophotic” or “mesophotic”, and “aphotic”. The bathymetric position of these light zones is variable and depends on water transparency and latitude, and they associate with the development of some autotrophic organisms. The range of modern seagrasses and, non-dasyclad green algae can be used to define the euphotic zone, and the deepest occurrence of *in-situ* red algae define the lower limit of the oligophotic zone (Pomar, 2001; Morsilli et al., 2012). In addition to light, nutrient availability also plays a major factor in controlling carbonate production and define as oligotrophic, mesotrophic, and eutrophic conditions (Hallock, 1987; 2015). Dupraz and Strasser (2002) discussed three main nutritional modes for Oxfordian coral- microbialite reefs of Swiss Jura (northern Tethys): phototrophic (light-dependent) associations which prevail in oligotrophic and pure carbonate settings, balanced photo-heterotrophic, and heterotrophic-dominated occur in association with siliciclastics input. According to some authors, the Upper Jurassic shallow coral buildups from northern Tethys were a phototrophic-dominated system, deposited in clear water with good light availability (Dupraz and Strasser, 2002; Martin-Garin et al., 2012). In contrast, microsolenid biostromes, associated with heterotrophic micro and macrofauna, developed in eutrophic condition (Insalaco, 1999), where the light penetration is usually low (meso-oligophotic zone). Stromatoporoids, the main bioconstructor of southern and intra- Tethys reefs during the Upper Jurassic, are considered to develop in shallow, high energy settings with strong to moderate oligotrophy conditions (Leinfelder et al., 2005). The stromatoporoid and mix stromatoporoid-coral buildups in the intra-Tethys show a high degree of debris production related to turbulence events. This reflects the importance of energy level and hydrodynamic processes in the formation of this kind of buildups.

The origin of turbulence in these systems has usually been related to storm events generated by surface waves. Recently, another source of turbulence has been highlighted in sedimentary systems linked to the internal waves and tides (Pomar et al., 2012; Shanmugam, 2013). Internal waves (IWs) are perturbations propagating along a pycnocline (e.g. Munk, 1981; Apel, 2002) and their breaking along continental margin and slopes creates episodic high- turbulence events which can remobilize the sediment and carry nutrients at the depth where the pycnocline intersects the sea floor (Leichter et al., 2003; Lamb, 2014; Arthur and Fringer, 2016; Woodson, 2018). However, the impact of internal waves in the sedimentary record and their effect on fossil communities has remained largely unrecognized. In carbonate systems, internal waves can provide two important factors for carbonate buildups to grow: food resources and water motion (Pomar et al., 2017). Furthermore, internal waves can resulted in deposition of high-energy facies associated with carbonate buildups dominated in low-energy settings (Pomar et al., 2012).

The debris-rich stromatoporoid facies were developed during the Late Jurassic-Early Cretaceous along the platform margin of Apulia Carbonate Platform (ACP). During this time, ACP was an isolated carbonate domain located in the eastern part of south Tethys (Figs.1; 2A). The previous studies of stromatoporoid-rich facies in ACP were mostly focused on sedimentological characteristics (Morsilli and Bosellini, 1997, Morsilli, 1998) and taxonomical interpretation (Russo and Morsilli, 2007). However, the factors controlling the development of these stromatoporoid buildups have been poorly studied. According to Russo and Morsilli, 2007, the stromatoporoids are mostly represented by *Ellipsactinia* sp. and *Sphaeractinia* sp. and they were developed along the external margin and proximal slope environments (Morsilli and Bosellini, 1997).

The platform margin of the ACP crops out in the Gargano Promontory and displays several units of marginal facies (Morsilli and Bosellini, 1997; Morsilli et al., 2017). The aims of this study are: 1- to analyse the facies distribution and lateral change of Upper Jurassic- Lower Cretaceous Monte Sacro Limestones (MSL), in order to reconstruct a depositional model for these stromatoporoid-rich units and, 2- to study the factors controlling the developments of the stromatoporoid buildups in MSL, including the potential role of internal waves as a possible source of episodic turbulence, resulted in extensive reef debris production.

2. Geological setting

The Apulia Carbonate Platform (ACP), one of the peri-Adriatic carbonate banks, was a major paleogeographic element of the southern margin of the Mesozoic Tethys Ocean (Fig. 2A). The ACP extended from the southeastern Abruzzi region across Apulia and the Strait of Otranto to the Greek islands of Cephalonia and Zante (Bosellini, 2002). This carbonate platform is the foreland of both the Apennine and the Dinaric thrust and fold belts (Bernoulli, 2001). It is bounded on both sides by basinal deposits. The western margin of the platform is downfaulted and buried underneath terrigenous sediments of the Apennine foredeep and the adjacent Apennine chain. Instead, the eastern margin of the platform lies 20–30 km offshore from the present Apulia Coastline in the Adriatic Sea (Bosellini et al., 1999; Borgomano, 2000; Morsilli et al., 2017). The ACP mainly consists of Upper Jurassic to Eocene shallow-marine carbonates, and in the Gargano Promontory and the Maiella Mountain also by the coeval slope to basin facies

(Bosellini et al., 1999; Borgomano, 2000; Bernoulli, 2001). The studied outcrops correspond to the Upper Jurassic- Lower Cretaceous Monte Sacro Limestones (MSL) (Fig. 2B) and they are located along the platform margin belt of the ACP, cropping out in the Gargano Promontory (Monte di Mezzo, Torre Mileto and Masseria Prencipe, Fig. 2C). The MSL in studied outcrops is characterized by massive limestones with stromatoporoids such as *Ellipsactinia* sp. and *Sphaeractinia* sp. (Morsilli and Bosellini, 1997; Russo and Morsilli, 2007). The outcropping Monte Sacro succession is about 300 m in the type section (Monte Sacro mountain) and has a stratigraphic distribution from Oxfordian to Berriasian (Pavan and Pirini, 1966; Luperto Sinni and Masse, 1994) and probably reaches the early Valanginian (Morsilli, 1998). Duo to the lack of biostratigraphic data from MSL successions in the studied intervals, the exact stratigraphic age range cannot be identified. However, the occurrence of *Calpionella* sp. near the top of the studied stratigraphic section (section A) can suggest an age interval between Tithonian to Berriasian (Bosellini and Morsilli, 1997).

3. Methods

The studied MSL outcrops are exposed along the platform margin belt of ACP in the Gargano area (Fig. 2C). Despite the limitation imposed by highly weathered outcrops of MSL in Gargano area, the interpretation of facies is possible along the surface of some outcrops where the quality of exposure surface allowed the study of distribution, organization, the shape of main biotas and characteristics of different facies. The Monte Sacro Limestones are well exposed in Monte di Mezzo section in the area of ~1.6 km long with a stratigraphic thickness of ~ 100 m (Fig. 3A). For investigation of lateral changes of facies, seven outcrops surfaces have been selected. The outcrops are characterized by m-thick massive limestone with no visible bedding surfaces and geometry. For vertical facies changes, one stratigraphic log has been measured and described. Sampling along the stratigraphic log (average one sample in every 5 m) complemented with sampling from the adjusted outcrops. In the other areas (Torre Mileto and Masseria Prencipe) the MSL are partially exposed as small outcrop windows. The described outcrop surfaces in Torre Mileto and Masseria Prencipe are arranged in cm to m-thick massive limestones (~ 2 m^2). The stromatoporoid lithofacies were recognized based on field description of stromatoporoids and corals with the identification of their growth forms. In order to study the internal sediments, a total number of 90 samples have been collected. All samples have been prepared for thin section analysis in order to study the textural characterization of internal sediments and identification of skeletal components. Components abundance was estimated based on point counting using the JMicroVision program and grouped in five categories: rare (less than 1%), present (2%–25%), common (26%–50%), abundant (51%–75%) and very abundant (76%–100%). The facies were identified according to Dunham (1962) and Embry and Klovan (1971). Light zonation of depositional environments (oligophotic, mesophotic and euophotic) and their relative boundaries has been defined following Pomar (2001) and Morsilli et al. (2012).

4. Results and interpretation

4.1. Facies description

On the basis of the lithology, rock texture, and components, three main lithofacies and four subfacies have been distinguished: LF1- stromatoporoid-rich facies (LF1-S1: floatstone with wackestone to fine-grained packstone, LF1-S2: rudstone to floatstone with intraclastic-bioclastic packstone-grainstone matrix), LF2- stromatoporoid- coral facies (LF2-S1: floatstone with wackestone to packstone matrix, LF2-S2: tabular stromatoporoids and coral with wackestone matrix), and 3- stromatoporoid- microbial facies (LF3). All lithofacies (LF1, LF2, LF3) can be recognized in Monte di Mezzo section where the lateral facies changes are visible (Fig. 3A). LF1 are the most exposed lithofacies (~ 1.2 km long) passes gradually to LF2 and basin-ward to LF3. Vertically, the stromatoporoid-rich facies (LF1) is the only lithofacies observed along the stratigraphic log (Fig. 3B). The LF1 is also recognized in small outcrops (~ 2 m^2) in Torre Mileto. The distribution of subfacies LF1-S1 and LF1-S2 on the surface of outcrops show a chaotic organization with sharp boundaries (Fig. 3C, D). In the vertical position, the LF1-S2 represented by rudstone- floatstone with intraclastic packstone to grainstone matrix, is developed at the base of the section while floatstone with wackestone to fine-grained packestone (LF1-S1) associated with *in-situ* stromatoporoids is more abundant at the top of section (Fig. 3B). stromatoporoid-coral facies (LF2) composed of cm to m- thick massive limestones exposed in Monte di Mezzo (LF2-S1) (Fig. 4A) and Masseria Prencipe (LF2-S2) (Fig. 4B). Stromatoporoid-microbial facies (LF3) recognized only in Monte di Mezzo section and characterized by m- thick massive limestones (Fig. 4C). The distribution of different lithofacies along the studied area shows that LF1 is the most abundant lithofacies (87.2%) followed by LF2 (11%) and LF1 (1.8 %) (Fig. 5A). In LF1, the debris-rich rudstone-floatstone (LF1-S2) is more frequent (62.7 %) than LF1-S1 (37.3 %) (Fig. 5B).

4.1.1. Stromatoporoid-rich facies (LF1)

In this facies the main biota and skeletal debris are represented by abundant cm to dm-sized stromatoporoids , minor corals, sponge-like organisms, chaetetids? and echinoid spines (Fig. 3 C). Two subfacies have been recognized (Fig. 6A, B, C): LF1-S1: stromatoporoid floatstone with wackestone to fine-grained packstone matrix (Fig. 6D), and LF1-S2- rudstone to floatstone with intraclastic-bioclastic packstone to grainstone matrix (Figs. 6 E, F). The LF1-S1 and LF1-S2 are co-existing within the stromatoporoid-rich facies (LF1), and they are separated by a sharp boundary (Fig. 6A, B, C). In LF1-S1, the dominant stromatoporoids taxa are *Sphaeractinia* sp. and *Ellipsactinia* sp. and they occur mostly in growth position (Figs. 7A, B, C). *In-situ* stromatoporoids show different growth forms as bulbous (Fig. 7A) columnar (Fig. 7B) and dendroid with robust branching (Fig. 7C). in some parts, the stromatoporoids with columnar shape can reach to 40 cm in diameter. The *Ellipsactinia* sp. has thicker lamellae and thinner inter-lamellar spaces compared with *Sphaeractinia* sp. where lamellae are thinner than inter-lamellar spaces or show the same size (Figs. 7C, D). The wackestone to packstone matrix composed of fine-grained peloids, very rare intraclasts as well as rare skeletal grains including bivavles, bryozoans and echinoids (Fig. 5F). The micro-encrusters such as *Tubiphytes-Crescentiella* are very common within the matrix and they mostly grew in association with stromatoporoids (Fig. 7F) or they developed in a nodule shape.

Subfacies LF1-S2 is characterized by cm to dm-sized intraclasts and fragments of stromatoporoids and corals distributed in a poorly-sorted packstone to grainstone matrix (Fig. 6D, E). The stromatoporoid clasts comprise mostly of *Sphaeractinia* sp. and *Ellipsactinia* sp. fragments. Other bioclasts including corals are characterized by fragments of phaceloid corals and predominantly enveloped by micro-encrusters such as *Tubiphytes- Crescentiella* (Fig. 6D). Other common bioclasts are fragments of micro-encrusters such as *Tubiphytes- Crescentiella*, *Radiomura cautica*, *Uvanella*?, and other undefined micro-encrusters. Rare components are bivalves, brachiopods, benthic foraminifers and echinoids. In the vertical position (section A) (Fig. 3 B), the number of debris rich LF1-S2, with abundant intraclast and bioclast components, decreases towards the top of the section where the mud-dominated LF1-S1 are commonly more developed.

4.1.2. Stromatoporoid- coral facies (LF2)

This Lithofacies is characterized by stromatoporoids (*Sphaeractinia* sp. and *Ellipsactinia* sp) and corals floated in a wackestone to packstone matrix (LF2-S1), and tabular stromatoporoids and corals associated with wackestone matrix rich in radiolarians (LF2-S2) (Figs. 4A, B). In Monte di Mezzo section, the LF2-S1occurs as massive limestones with abundant fragments and *in-situ* *Ellipsactinia* sp., *Sphaeractinia* sp., other undefined stromatoporoids and corals colonies that mostly preserved in life position (Fig. 4A; 8A). The dominant morphology of corals is branching (phaceloid), with coral colonies ranging from 10 up to 80 cm in diameter and up to 50 cm in height (Fig. 8 A). The coral branches are mainly delicate, but the robust form is also present (Fig. 8 B). The branches touched each other's, leaving a very thin space in between (Fig. 8 C, D, F). The internal sediments between stromatoporoids and corals composed of mm-sized bioclasts distributed in a wackestone to packstone (Fig. 9A, B). The non-skeletal grains are peloids and rare amount intraclasts. The bioclasts are debris of echinoids, bivalves and gastropods and some pelagic components such as *Saccocoma* sp. (Fig. 9C). The skeletal debris are usually micritized or enveloped by micrites. The micro-encrusters are commonly represented by *Tubiphytes-Crescentiella* which occur mostly as nodules or in growth form by growing on other biotic components (Fig. 9D). The fragments of *Tubiphytes- Crescentiella* are also present.

In the lower part of Masseria Prencipe, the LF2-S2 shows different characteristics. *Ellipsactinia* sp. and *Sphaeractinia* sp. are completely absent in this area. Instead, *in-situ* and tabular form stromatoporoid colonies were developed in association with corals (Fig. 4B). The stromatoporoid colonies reach 50 cm in height and up to 60 cm in diameter (Fig. 10 A), and characterized by thick and continuous lamellae which envelope each other's (Fig. 10 A). The stromatoporoid colonies are associated with cm-sized *in-situ* phaceloid coral colonies (Fig. 10B). The internal sediments are characterized by dark muddy wackestone matrix with main components represent by radiolarians (Fig. 10C). The radiolarians are mostly dissolved and replaced by fine-grained dolomites. (Fig. 10C).

4.1.3. Stromatoporoid- microbial facies (LF3)

This lithofacies occur in massive limestone and crops out only in one outcrop in Monte di Mezzo section (Fig. 3A; 4C). The lithofacies is characterized by *in- situ* stromatoporoids surrounded by wackestone to fine-grained packstone and developed on the top of discontinuous dm-sized of stromatolite-like structures (Fig. 4C; 11A, B). The stromatoporoids taxa represent by *Ellipsactinia* sp. and *Sphaeractinia* sp. and *Cylicopsis* sp? (Fig. 11C). These biotic components are associated with fragments of sponge- like organisms and echinoid spines. The other components within the matrix are fragments of gastropods, foraminifers and micro-encrusters such as *Tubiphytes- Crescentiella* and *Radiomura cautica.* Under the microscope, the internal fabric of stromatolite-like structures can be distinguished from the stromatoporoids (Fig. 11 D, E). The stromatolite-like fabric is characterized by alternating micritic dark laminae and clear laminae composed of microgranular calcite cements (Fig. 11E). Geopetal fabrics are present in some cavities and characterized by fine-grained internal sediment fillings at the base and sparry calcite at the top of cavities.

4.2. Depositional environments interpretation

In the Gargano Promontory during the Late Jurassic, the Apulia Carbonate Platform (ACP) was a part of a carbonate bank passing downslope to the Adriatic Basin. The MSL represent deposition in the distal part of margin and it characterized by the development of stromatoporoid facies with some branching corals. The external margin passes gradually to clinostratified slope facies of Ripe Rosse Formation with breccia and calciturbidites, passing basinward to pelagic mudstone with chert of the Maiolica Formation (Morsilli and Bosellini, 1997). The model proposed by these Authors is a sort of a distally steepened ramp, with an inclination of 5-10 degree associated with the external part of margin (Fig. 12).

According to this general model, the three main lithofacies here distinguished, stromatoporoid-rich facies, stromatoporoid- coral facies and stromatoporoid- microbial facies, represents the external margin from the proximal zone to the more distal part, respectively (Fig. 13). Despite the limitations imposed by the limited lateral continuity of the studied outcrops and lack of depositional geometry, the general interpretation of the lithofacies has been made on the basis of skeletal components and textures. The bathymetric position of lithofacies can be estimated by recognition of components adapted to different light zones (euphotic, mesophotic and oligophotic).

Stromatoporoid-rich facies (LF1) mainly consists of stromatoporoids such as *Ellipsactinia*, *Sphaeractinia* with bulbous, dendroid, branching and columnar shape (Fig.13). The stromatoporoids are characterized by enveloping growth bands (Fig. 7A-C) . Based on James and Bourque (1992), these growing form of stromatoporoids can adapt to quite to moderate water energy.

In LF1, the *in-situ* stromatoporoids are close but not densely stacked nor in contact. So, they could not build a rigid framework reef (Fig. 3C). These characteristics fit the “close cluster” reef type of Riding (2002). These matrix-supported reefs are characterized by deposition in low-energy environments where they can develop large size and moderate relief buildups (Riding, 2002). This close cluster reefs, despite the deposition in quiet environments, are mainly prone to high-energy hydrodynamic events, but the close arrangement of skeletons may prevent the high-energy events to remove and sorting the internal sediments (Riding, 2002). The internal sediments in stromatoporoid-rich buildups are represented by wackestone to fine-grained packstone (LF1-S1) (Fig. 6D) and packstone to grainstone (LF1-S2) (Fig. 6E, F). This indicates that LF1 can be developed under different energy conditions. The wackestone to fine-grained packstone matrix (LF1-S1) between *in-situ* stromatoporoids (Fig. 6D) shows that this kind of organisms grew in low-energy and quiet environments. Figure 3B shows that *in-situ* stromatoporoids associated with wackestone matrix (LF1-S1) are better developed at the top of Monte Sacro section (section A) where the hydrodynamic energy is low due to possible sea-level rise. *Tubiphytes* sp. is the dominant micro-encruster which directly developed on the surface of stromatoporoids (or other hard substrates) (Fig.7F). The absence of *in- situ* light-dependent micro-encrusters such as *Lithocodium- Bacinella* and development of heterotrophic micro-encrusters (*Tubiphytes* sp.) indicates that this subfacies can be developed in mesophotic conditions where the light is not enough for phototrophic micro-encrusters to grow. The LF1-S1 is in association with intraclastic-bioclastic packstone-grainstone (LF1-S2). In this subfacies, the occurrence of cm-sized angular intraclasts and bioclasts in a poorly-sorted packstone-grainstone (Fig. 6E, F) indicates that LF1-S2 were deposited under high-energy conditions. The intraclast and bioclast debris are only sourced from the current lithofacies (LF1) (clasts of stromatoporoids, corals and micro-encrusters). The angular intraclasts associated with poorly-sorted packstone-grainstone indicate that the hydrodynamic energy was not continuous enough to improve the roundness and sorting of the sediments. The characteristics and origin of internal sediments suggest that stromatoporoids were mainly developed in low-energy environments (LF1-S1) where the energy was not enough to build a rigid framework (close cluster fabric), then the buildups were affected by episodic high-energy events resulted in the accumulation of high-energy deposits (LF1-S2). This also can interpret the chaotic organization of LF1-S1 and LF1-S2 in stromatoporoid-rich facies in MSL (Fig. 6 A, B, C). This lithofacies were deposited in proximal zone of external margin (Fig. 13).

In stromatoporoid-coral facies (LF2) the *in-situ* phaceloid corals are characterized by delicate branching shape, suggesting that these corals can be thrived in relative low- energy environments. Also, Dupraz and Strasser (2002) discussed that corals with phaceloid morphology could be adapted to soft substrates and thrived in high sedimentation rates and quiet environments. In LF2-S1, the stromatoporoids and corals are floated in a matrix without building a wave-resistance rigid framework. This fits the characteristics of "cluster reef" and indicates the deposition in relative quiet conditions (Riding, 2002). The internal sediments represent by bioclast wackestone and packstone matrix (LF2-S1) suggest that corals and stromatoporoids were developed in relative moderate to low-energy environments. Micritization of skeletal debris and rare amounts of intraclasts suggests low hydrodynamic conditions. Also, the absence of light-dependent organisms such as *Lithocodium- Bacinella* and dasyclad green algae can indicate the deposition in limited-light conditions (mesophotic).

In LF2-S2, the stromatoporoids developed laminar to tabular shape morphology (Fig.10A). Compare with Devonian stromatoporoids, this kind of growth form can develop in deeper and quiet waters (Kershaw, 1998). The coral colonies are represented by phaceloid form, suggesting deposition in quite environments (Dupraz and Strasser, 2002). The internal sediments associated with stromatoporoids and corals in LF2-S2 are characterized by wackestone matrix rich in radiolarian. This indicates the deposition of this subfacies in more distal margin under low-energy conditions. This lithofacies were developed between proximal and distal part of external margin (Fig.13).

The stromatoporoid- microbial facies (LF 3) is characterized by stromatolite-like structures accompanied by stromatoporoids in growth position. Stromatolites are known to form in marginal marine, shallow and deep subtidal and basinal environments (Flügel, 2004). In the Upper Jurassic, the microbial-dominated reefs were mostly grown in deep and low energy environments where the sedimentation rate was very low (Leinfelder et al., 1996; Schmid, 1996). On the top of stromatolite-like laminae, the internal sediments between stromatoporoids are wackestone to fine-grained packstone showing that in this lithofacies the stromatoporoids were developed in relative low-energy environments. This lithofacies were deposited in the distal part of external margin (Fig.13).

5. Discussion

5.1. Other examples from South and intra-Tethys reefs

In the intra-Tethys and southern part of Tethys, Upper Jurassic reefs are quite common. The sedimentological characteristics of this kind of reefs have been described in Italy: Central Apennines (Rusciadelli et al., 2011) and NW Sicily (Basilone and Sulli, 2016a), Slovenia (Turnšek et al., 1981), Austria: Northern Calcareous Alps (Schlagintweit and Gawlick, 2008); and in Czech Republic (Hoffmann et al., 2017). In Arabian Plate, the Upper Jurassic facies are reported from Saudi Arabia (Al-Awwad and Pomar, 2015, Rosales et al., 2018) and Iran (Kano et al., 2007).

In central Apennines of Italy, (Rusciadelli et al., 2011) have been studied the different reef units developed in Ellipsactinia Limestones. These units represent by coral and Chaetetids Unit (CCU), corals and stromatoporoids unit (CSU), and the stromatopores unit (SSU). These units were deposited along three main reef zones 1- coral and Chaetetids Unit was deposited in an internal and protected deep back-reef- lagoon, 2- corals and stromatoporoids unit were developed in a reef flat, and 3- stromatopores unit which occur in an external and shallow zone. In SSU unit of Ellipsactinia Limestones, the stromatoporoids are surrounded by bio-lithoclastic sediments. This shares similarity with LF1-S2 in MSL where debris-rich subfacies developed in association with stromatoporoid-rich facies (LF1). However, the stromatopores unit in Ellipsactinia Limestones described being deposited along the shallowest part of margin and with high energy conditions, while in MSL this facies placed in the deeper part of margin, in more quiet environments with an episodic source of high energy events.

In NW Sicily, Basilone and Sulli (2016a) described the upper Tithonian–Valanginian carbonate facies distribution along a tectonically controlled rimmed carbonate shelf. A reef complex is composed of inner reef flats which characterized by corals. The outer zone (reef wall) were dominated by *Ellipsactinia* sp. boundstone, and toward sea direction, the encrusters were well developed. In the deeper part of the platform (fore- reef), breccia and calcarenites were deposited as clinoforms passing deep-ward to calpionellids limestone. In *Ellipsactinia* boundstone facies the internal sediments are ranging from intraclastic breccia to bioclast packstone to grainstone. The *Ellipsactinia* sp. is characterized by densely packed clusters and quasi-rigid mound-shaped structures which suggest the deposition of this zone under high-energy hydrodynamic conditions (Basilone and Sulli, 2016a). The *Ellipsactina* sp. reefs are developed as matrix of the Upper Tithonian–Valanginian breccias described by Basilone et al. (2016b). The stromatoporoid-rich facies (LF1) of MSL is comparable with *Ellipsactinia* boundstone described here by Basilone and Sulli (2016a). In both examples, the main biotic components are stromatoporoids (*Ellipsactinia* sp.) surrounded by intraclastic rich sedimends (LF1-S2). However, in MSL the LF1 interpreted to be developed in low-energy environments hitting by episodic high-energy events.

The Upper Jurassic reefs represent by *Ellipsactinia* limestones have also been reported from Friuli Platform, southern Alps (Italy) by Cati et al. (1987) and Picotti and Cobianchi (2017). These studies are mostly focused on the stratigraphic interpretation of Upper Jurassic- Lower Cretaceous successions. In this area, the *Ellipsactinia* limestones considered to be real reef sequences, and they were grown along the margin of Friuli Platform.

Schlagintweit and Gawlick (2008) studied the Upper Jurassic- basal Cretaceous shallow-water carbonates in Northern Calcareous Alps, Austria, and described as the main reef body a micro-encruster boundstones with a variable amount of cement crusts. This platform is characterized by a steep margin, and the reef facies occurs in a fore-reef slope environment, with coral-stromatoporoid patch-reefs and monotypic microsolenid floatstone. Instead, the *Ellipsactinia* wackestone facies is associated with platform margin and upper slope. In this example, *Ellipsactinia*-rich facies were associated with wackestone, showing the depositional of this facies in quiet and low energy conditions. The *Ellipsactinia* wackestone facies described by Schlagintweit and Gawlick (2008) can be comparable with stromatoporoid-rich facies (LF1) in MSL where the stromatoporoids are surrounded by wackestone to fine-grained packstone matrix (LF1-S1).

Turnšek et al. (1981) studied the Oxfordian- lower Kimmeridgian reef complex of north-western ex-Yugoslavia (Croatia). This reef complex is interpreted as a classical barrier reef, with all the typical sub-environments, from the lagoon to the basin. The main reef is subdivided into *Actinostromarid zone* which is dominated by stromatoporoids and a *Parastromatoporoid zone* which is characterized by coral- chaetetids facies. The back reef corresponded to a lagoon with patch reefs and defined as a *Cladocoropsis* zone. The stromatoporoid-rich facies (LF1) of MSL are comparable with *Actinostromarid zone* which located in the shallow central reef. The sediments between biocounstructors contain debris of breccia and calcarenite, which suggest this facies to develop in very high energy settings. However, in this zone, on the contrary with LF1 in MSL, the corals are well developed.

Hoffmann et al. (2017) studied the Tithonian–lower Berriasian of Štramberk reef complex, Czech Republic. These reefs were developed on an isolated intra- Tethys carbonate platform. Two main boundstone types have been recognized. A- Coral- microbial boundstone attributed to a low-energy setting and composed mostly of branching corals associated with light- dependent micro-encrusters (*Lithocodium- Bacinella*), and B- micro-encruster-cement boundstone that corresponds to the high-energy setting of an upper fore-reef slope environment. This facies is characterized by the presence of micro-encrusters accompanied by synsedimentary cements and absence of corals and light-dependent micro-encrusters like *Lithocodium- Bacinella.* In this research the corals considered to be the main metazoan reef builders outcompeted stromatoporoids. This can be an exception for reefs developed in intra-Tethys realms including MSL in Apulia Platform.

In the Arabian Plate, Al- Awwad and Pomar (2015) studied the origin of rudstone- floatstone beds in the Upper Jurassic Arab-D reservoir, instead Rosales et al. (2018) described the distribution of microfacies along this carbonate ramp. The middle ramp setting is defined by a reef belt with microbial-stromatoporoid- coral buildups which are characterized by the presence of coral and stromatoporoids in a wackestone to grain-dominated packstone matrix. Microbial fabrics are mostly thrombolite and microbial filaments. In the Zagros Basin, Iran, Kano et al. (2007) reported stromatoporoid biostromes during Tithonian. The stromatoporoids are associated with corals and calcareous algae showing rudstone to floatstone texture. On the contrary respect to the Arab-D the interpreted depositional environment is as a back-reef lagoon. The last two examples from Saudi Arabia and Iran show that in this part of southern Tethys, stromatoporoid-rich buildups can be developed along the different part of a carbonate platform profile, while corals were less developed. This shares the similarity with other stromatoporoid-rich facies that occur in other south and intra-Tethys realms and partially the interpreted setting of the Apulia Platform. However, in intra-Tethys area stromatoporoids are represented by *Ellipsactinia* sp. and *Shpaeractinia* sp., as in MSL.

5.2. Factors controlling the MSL reef development

Development of carbonate buildups is strongly related to different factors including nutrient and light availability, hydrodynamic energy and sedimentation rate (Mutti and Hallock, 2003; Pomar et al., 2012, 2017). Among these factors, the nutrient source and light availability was the most important factor which resulted in the formation of different buildups in Upper Jurassic. The comparison of the factors controlling the development of MSL reefs with northern Tethys reefs is shown in figure 14.

Dupraz and Strasser (2002) discussed the nutritional modes required for Oxfordian coral-microbialite reefs growth in Swiss Jura. Reefs with light-dependent, phototrophic-dominated fauna were developed in nutrient-poor, pure carbonate environments. Balanced phototrophic-heterotrophic reefs fauna were prevalent in mixed siliciclastic-carbonate environments. In this condition the development of light-dependent micro-encrusters such as *Lithocodium- Bacinella* is limited. With the increase of terrigenous input, the water alkalinity will enhance and together with nutrients, an ideal condition for the growth of microbialites can be occurred favouring the condition for the development of the heterotrophic-dominated type reefs (Fig.14).

In the Apulia Platform all the stromatoporoid-rich facies are developed in a carbonate environment without evidence of terrigenous input (Fig.14). The phototrophic-dominated faunas are represented by the presence of corals in stromatoporoid- coral facies. However, the abundant presence of organisms such as echinoids in all studied facies (LF1, LF2, LF3), the absence of light-dependent micro-encrusters (e.g. *Lithocodium- Bacinella*) on the surface of organisms, and the developments of microbial facies in LF3, make these buildups fall within the phototrophic-heterotrophic reefs (*sensu* Dupraz and Strasser, 2002) (Fig.14).

Olivier et al. (2004) studied the middle and late Oxfordian coral-microbialite reefs of northeastern France and argued that microbialites mostly grow in mesotrophic conditions in mixed siliciclastic-carbonate environments. In this setting, the light-dependent micro-encrusters (e.g. *Lithocodium*) were rare showing the poor light availability favoured by this kind of organisms. In pure carbonate environments, a low microbialite amount can be developed on phototrophic coral communities in oligo- mesotrophic conditions (Olivier et al., 2007). Also, San Miguel et al. (2017) studied the Kimmeridgian metazoan to microbial-dominated buildups in the shallow ramp of the Iberian basin, Spain. The author discussed the formation of microbial buildups under high nutrient levels. In MSL, the microbialites grown in a pure carbonate environment and they have not strongly developed in the studied facies. As a result, they may be assumed to be formed in an oligo- mesotrophic conditions as discussed by Olivier et al. (2007). While an increase of nutrient level can act as a factor limiting penetration of light, the stromatoporoids buildups associated with microbialites can be adapted to mesophotic environments. In the Upper Jurassic reefs, siliceous sponge mound, pure microbialites and microsolenid biostromes reefs we adapted to high nutrient levels (eutrophic) and poor light (oligophotic) (Insalaco, 1996; Olóriz et al., 2003; Leinfelder et al., 2002). There is no evidence of formation of this kind of organisms in MSL. The other important factor in Upper Jurassic reef development is hydrodynamic energy. The coral reefs in northern Tethys can expand in high energy condition, and they are mostly associated with high energy facies (e.g. rudstone-floatstone) (Dupraz and Strasser, 2002). In mid-ramp setting, Olivier et al. (2011) reported coral-microbialite reefs developed under low energy conditions. These coral- microbialite reefs influenced by episodic high energy events evidenced by coarse bioclastic interbeds. This can be a case for MSL, where the *in-situ* stromatoporoids developed in quiet conditions (LF1-S1) and hit by episodic high-energy events resulting in the formation of debris rich facies (LF1-S2). Unlike Late Jurassic stromatoporoids, paleoecological and morphological characteristics of Palaeozoic stromatoporoids received more attention in literatures (e.g., Kershaw, 1998; Da Silva et al., 2011a, b; Corlett and Jones, 2011; Kershaw et al., 2013; Kershaw and Mõtus, 2016; Jakubowicz et al., 2018). Based on Kershaw (1998), in low-nutrient and oligotrophic conditions, the stromatoporoids can develop large bioherms and biostromes while in mesotrophic conditions the small bioherms are more likely to be developed. In the case of MSL the stromatoporoids did not build a high relief buildups or rigid framework (Fig. 3C). This indicates that stromatoporoid-rich buildups in MSL could be developed under the mesotrophic conditions.

In MSL, stromatoporoid- coral facies (LF2) indicates grow of stromatoporoids and corals in a similar setting. This kind of stromatoporoid- coral intergrowths is also reported from Devonian stromatoporoid- coral buildups. Corlett and Jones (2011) studied the Devonian stromatoporoid-dominated and coral-dominated reefs in the Mackenzie Basin, Canada, and they argued that coral-stromatoporoid intergrowth is adapted to a transitional ecological zone between two main buildups. Da Silva et al. (2011a) demonstrated that stromatoporoid and corals could grow into an association without any negative impact on each other growth. Corals can be also grown on the dead part of stromatoporoids and *vice versa*. In MSL, the *in-situ* growth of branching form corals associated with stromatoporoids suggests that this form of corals can generate in ecological conditions close to the stromatoporoids. This zone can be equivalent to transitional zone argued by Leinfelder et al. (2005), for environmental ranges of Upper Jurassic stromatoporoids and corals, which placed the stromatoporoid- corals intergrowths in moderate oligotrophy conditions which can be reached to mild mesotrophy in the case of MSL (Fig. 14).

5.3. Origin of turbulence event- the impact of internal waves

High energy reefs, rich in debris and poor in micrite, were developed during the Late Jurassic time in north and southern part of Tethys (Leinfelder et al., 2002). In MSL, the stromatoporoid-rich facies (LF1) consist of low-energy deposits associated with stromatoporoids (LF1-S1). These low-energy facies are embedded with poorly sorted rudstone to floatstone with intraclastic-bioclastic packstone-grainstone debris (LF1-S2). This indicates that stromatoproid-rich buildups in MSL were affected by range of episodic high-energy events, interpreted as storm-events (Morsilli and Bosellini, 1997). The key point is to explain the source of episodic high energy turbulence in a context of relatively deep water. In the literature, generally the high energy events are explained as the effect of surface storm waves. This storm waves generate turbulence (Ager, 1974) and occur in the shallow part of shelf and coastal zone and they can move the eroded sediments in the direction of the wind, causing erosion, and down-dip transport, and re-deposition of sediments known as tempestites (Immenhauser, 2009). However, the characteristics of intraclastic- bioclastic rudstone- floatstone debris (LF1-S2) in the MSL do not fit in the context of surface storm waves deposits because 1- the most components and clasts are related to the same depositional setting (e.g., clasts of stromatoporoids, corals, and microbialites), and 2- there are no shallow water components or clasts associated with debris.

In this context, internal waves can be a good candidate for the possible source of episodic storms in stromatoporoid buildups of MSL. Internal waves (IWs) are waves perturbations propagating along the interface of two density-stratified fluids (Pycnocline) (e.g., Munk, 1981; Apel, 2002 among others). The depth of pycnocline commonly occur at the mid-shelf setting when it related to seasonal thermocline (shallow pycnocline), or it can occur at deeper depths when it is associated with permanent thermocline (Butman et al., 2006; Pomar et al., 2012) (Fig. 15). Internal waves can cause episodic high turbulence events at any depth where pycnocline intersect the sea floor. As a result, these IWs can remobilize, rework and re-deposited the sediments in both down-dip and up-dip direction (Pomar et al., 2012; Morsilli and Pomar, 2012; Bádenas et al., 2012).

In carbonate systems, internal waves are also an important mechanism for distribution of nutrients, planktons and larvae associated with thermal variation as a result of vertical movement of the thermocline (Pomar et al., 2012). Pycnocline is associated with the zone of internal wave propagation and high nutrient availability (Fig. 15), and therefore suspension-feeder metazoans can produce buildups at this depth (Pomar et al., 2017). This can be an explanation for the reason that most Phanerozoic buildups developed in the mid-shelf setting.

As discussed before the *in-situ* stromatoporoid buildups (LF1-S1) in MSL can be developed under mesophotic conditions in low-energy ambients (Fig. 15). In these quiet environments, the generation of debris-rich stromatoporoids facies (LF1) in MSL can be summarized as the following stages (Fig. 16).

Stage A) growth of the stromatopotoids (LF1-S1) : in this stage the stromatoporoids can grow on a mud-dominated substrate under low-energy and mesophotic conditions (Fig. 16A).

Stage B) development of debris-rich facies of LF1-S2: during this period, high energy internal waves hit the stromatoporoid buildups developed in the stage A (Fig. 16B) . The debris of stromatoporoids, corals, and other biota can be generated as a result of high-energy event produced by internal waves (intraclastic-bioclastic packstone-grainstone) . These debris can be placed between the big fragments of LF1-S1 and resulted in chaotic arrangement of LF1-S1 and LF1-S2 in stromatoporoid-rich facies (LF1) (Fig. 3C, D). During this step, the internal waves can also bring nutrient-rich waters to the buildups.

Stage C) re-generation of stromatoporoids (LF1-S1) in this phase, the quiet condition between two high-energy events allowing precipitation of mud again (Fig. 16 C). The amount of nutrients provided by internal waves during stage B, is sufficient for stromatoporoids to re-generate again under low-energy condition of this stage before hitting by internal waves in the next stage (stage B).

The effect of internal waves on the formation of high energy rudstone- floatstone facies has also been reported from other parts of Tethys (Alnazghah et al., 2013; Al-Awwad and Pomar, 2015). Alnazghah et al. (2013) reported the development of high energy intraclastic–bioclastic rudstone-floatstone facies associated with flank facies of pinnacles in carbonate ramp of Iberian basin, Spain (western Tethys). These pinnacles were occurred in mud-dominated settings, below the wave- base level. In this case, the occurrence of high energy, coarse-grained flank facies in a context of low-energy ambient conditions reported as a paradox that solved by interpretation of the internal waves as a possible source of turbulence to explain the origin of the flank facies. Comparing with MSL, the main difference is the type of metazoans which in MSL the biota are represented by stromatoporoids but in Iberian basin the corals are the main mezatoans. However, this example shares similarities with the MSL. 1- In Monte Sacro limestones, the *in-situ* stromatoporoids are mostly surrounded by wackestone to fine-grained packstone (LF1-S1) which is comparable with the Iberian basin where the metazoans are distributed a mud-dominated matrix. 2- The occurrence of high energy intraclastic- bioclastic rudstone- floatstone facies (LF1-S2) in low-energy environments in MSL is comparable with Iberian basin where the high-energy flank facies occurred in a quiet environment, which in both cases can be interpreted as a result of internal waves. Al- Awwad and Pomar (2015), studied the origin of the rudstone-floatstone beds in Upper Jurassic Arab- D Formation, Saudi Arabia. The authors proposed a ramp depositional settings where the outer ramp was dominated by deposition of muds, interbedded with high energy rudstone- floatstone deposits. In this case, the generation of these high-energy beds in a context of low energy ambient interpreted to be a result of internal waves. This is compatible with the condition of occurrence of intraclastic-bioclastic debris (LF1-S1) in the case of MSL. However, in this example, the rudstone- floatstone beds were deposited in deeper part of the ramp where no associated buildups reported.

6. Conclusion

1- Along the deeper part of upper Jurassic- lower Cretaceous marginal facies of Monte Sacro Limestone, Gargano Promontory (southern Italy), three main lithofacies have been distinguished: LF1- stromatoporoid-rich facies, LF2- stromatoporoid-coral facies, and LF3- stromatoporoid- microbial facies. Stromatoporoid-rich facies (LF) are characterized by abundant growth of *Ellipsactinia* sp. and *Sphaeractinia* sp. in a low-energy mud-dominated matrix (wackestone to fine-grained packstone) (LF1-S1) with embedded rudstone-floatstone within higher energy intraclastic-bioclastic packstone-grainstone (LF1-S2). The organization of stromatoporoids, matrix-dominated fabric and lack of rigid framework share the characteristics of cluster reefs. Toward basin, a range of branching coral colonies is associated with stromatoporoids mainly *Ellipsactinia* sp. and *Sphaeractinia* sp. (LF2) distributed in wackestone to packstone matrix (LF2-S1) and tabular form stromatoporoids and corals occur within a wackestone matrix rich in radiolarian (LF2-S2). In the deeper part of margin, the stromatoporoids accompanied with stromatolite-like mats (stromatoporoid- microbial facies) and surrounded by wackestone to fine-grained packstone.

2- Nutrients and light availability as well as hydrodynamic energy, are the most important factors controlling the development of this type of buildups during the Late Jurassic. In Monte Sacro Limestones, a mild oligotrophy to moderate mesotrophy condition is proposed for stromatoporoid-rich buildups. The lack of light-dependent components in studies facies shows that the light penetration was not enough and the stromatoporoid-rich buildups were developed in pure carbonate environments in a mesophotic settings.

3- In Monte Sacro Limestone, as well as other intra-Tethys stromatoporoid-dominated facies, the high amount of debris-rich facies indicates that these buildups were prone to a range of episodic high-energy events. While no evidence of surface storm waves has been seen (lack of shallow depth components), the turbulence events can be related to internal waves. Internal waves affected the buildups in two main ways: producing the debris-rich facies of LF1-S2 and pumping the nutrients needed by metazoans (mainly stromatoporoids) to grow (LF1-S1) . These effects can be also found in other carbonate systems developed during other geological time intervals.

Acknowledgement

This work is a contribution to the research projects FAR 2016 and 2017 – Università degli Studi di Ferrara (M.M.). We also acknowledge Renzo Tamoni for thin sections preparation. We would like to thank Felix Schlagintweit for identification of some micro-encrusters fossils name. The authors are also grateful to Prof. Beatriz Bádenas and anonymous reviewer whose comments greatly improved the manuscript.

References

Ager, D. V, 1974. Storm deposits in the Jurassic of the Moroccan High Atlas. Palaeogeography, Palaeoclimatology, Palaeoecology 15, 83–93. https://doi.org/https://doi.org/10.1016/0031-0182(74)90026-1.

Alnazghah, M.H., Bádenas, B., Pomar, L., Aurell, M., Morsilli, M., 2013. Facies heterogeneity at interwell-scale in a carbonate ramp, Upper Jurassic, NE Spain. Marine and Petroleum Geology 44, 140–163. https://doi.org/10.1016/j.marpetgeo.2013.03.004

Apel, J.R., 2002. Oceanic internal waves and solitons. In: Jackson, C.R. (Ed.), An Atlas of Oceanic Internal Solitary Waves. Global Ocean Associates. Prepared for Office of Naval Research - Code 322 PO, Alexandria, VA, pp. 1–40

Arthur, R.S., Fringer, O.B., 2016. Transport by breaking internal gravity waves on slopes. Journal of Fluid Mechanics 789, 93-126. doi:10.1017/jfm.2015.723

Al-Awwad, S.F.A., Pomar, L., 2015. Origin of the rudstone–floatstone beds in the Upper Jurassic Arab-D reservoir, Khurais Complex, Saudi Arabia. Marine and Petroleum Geology 67, 743–768. https://doi.org/10.1016/j.marpetgeo.2015.05.014

Bádenas, B., Aurell, M., 2010. Facies models of a shallow-water carbonate ramp based on distribution of non-skeletal grains (Kimmeridgian, Spain). Facies 56, 89–110. https://doi.org/10.1007/s10347-009-0199-z

Bádenas, B., Pomar, L., Aurell, M., Morsilli, M., 2012. A facies model for internalites (internal wave deposits) on a gently sloping carbonate ramp (Upper Jurassic, Ricla, NE Spain). Sedimentary Geology 271–272, 44–57. https://doi.org/10.1016/j.sedgeo.2012.05.020

Basilone, L., Sulli, A., 2016a. A facies distribution model controlled by a tectonically inherited sea bottom topography in the carbonate rimmed shelf of the Upper Tithonian–Valanginian Southern Tethyan continental margin (NW Sicily, Italy). Sedimentary Geololgy 342, 91–105. https://doi.org/10.1016/j.sedgeo.2016.06.013

Basilone, L., Sulli, A., Gasparo Morticelli, M., 2016b. Integrating facies and structural analyses with subsidence history in a Jurassic–Cretaceous intraplatform basin: Outcome for paleogeography of the Panormide Southern Tethyan margin (NW Sicily, Italy). Sedimentary Geology 339, 258–272. doi:10.1016/j.sedgeo.2016.03.017

Bernoulli, D., 2001. Mesozoic-Tertiary carbonate platforms, slopes and basins of the external Apennines and Sicily, In: Vai, G.B., Martini, I.P. (Eds.), Anatomy of an Orogen: The Apennines and Adjacent Mediterranean Basins. Springer Netherlands, Dordrecht, pp. 307–325. https://doi.org/10.1007/978-94-015-9829-3_18

Borgomano, J.R.F., 2000. The Upper Cretaceous Carbonates of the Gargano-Murge Region, Southern Italy: A Model of Platform-To-Basin Transition. American Association of Petroleum Geologists Bulletin 84, 1561. https://doi.org/10.1306/8626BF01-173B-11D7-8645000102C1865D

Bosellini, A., 2002. Dinosaurs "re-write" the geodynamics of the eastern Mediterranean and the paleogeography of the Apulia Platform. Earth-Science Reviews 59, 211–234. https://doi.org/10.1016/S0012-8252(02)00075-2

Bosellini, A., Morsilli, M., 1997. A Lower Cretaceous drowning unconformity on the eastern flank of the Apulia Platform (Gargano Promontory, southern Italy). Cretaceous Research. 18, 51–61. https://doi.org/https://doi.org/10.1006/cres.1996.0049

Bosellini, A., Morsilli, M., Neri, C., 1999. Long-Term Event Stratigraphy of the Apulia Platform Margin (Upper Jurassic To Eocene, Gargano, Southern Italy). Journal of Sedimentary Research 69, 1241–1252. https://doi.org/10.2110/jsr.69.1241

Bosscher, H., Schlager, W., 1992. Computer simulation of reef growth. Sedimentology 39, 503–512.

Butman, B., Alexander, P.S., Scotti, A., Beardsley, R.C., Anderson, S.P., 2006. Large internal waves in Massachusetts Bay transport sediments offshore. Continental Shelf Research 26, 2029–2049.

Catalano, R., D'Argenio, B., 1981. Paleogeographic evaluation of a continental margin in Sicily. Guidebook, Penrose Conference, Controls of Carbonate Platform Evolution, Palermo, Italy. p. 142.

Cati, A., Sartorio, D., Venturini, S., 1989. Carbonate platforms in the subsurface of the northern Adriatic Sea. Memorie della Società Geologica Italiana 40, 295–308.

Cecca, F., Martin Garin, B., Marchand, D., Lathuiliere, B., Bartolini, A., 2005. Paleoclimatic control of biogeographic and sedimentary events in Tethyan and peri-Tethyan areas during the Oxfordian (Late Jurassic). Palaeogeography, Palaeoclimatology, Palaeoecology 222, 10–32. https://doi.org/10.1016/j.palaeo.2005.03.009

Corlett, H., Jones, B., 2011. Ecological controls on Devonian stromatoporoid-dominated and coral-dominated reef growth in the Mackenzie Basin, Northwest Territories, Canada. Canadian Journal of Earth Sciences 48, 1543–1560. https://doi.org/10.1139/e11-056

Da Silva, A.C., Kershaw, S., Boulvain, F., 2011a. Sedimentology and stromatoporoid palaeoecology of Frasnian (upper Devonian) carbonate mounds in southern Belgium. Lethaia 44, 255–274. https://doi.org/10.1111/j.1502-3931.2010.00240.x

Da Silva, A.C., Kershaw, S., Boulvain, F., 2011b. Stromatoporoid palaeoecology in the Frasnian (Upper Devonian) Belgian platform, and its applications in interpretation of carbonate platform environments. Palaeontology 54, 883–905. https://doi.org/10.1111/j.1475-4983.2011.01037.x

Dercourt, J., Gaetani, M., Vrielynck, B., Barrier, E., Biju, Duval B., Brunet, M.F., Cadet, J.P., Crasquin, S., Sandulescu, M., 2000. Atlas Peri-Tethys, Paleogeographical Maps. CCGM/CGMW, Paris, pp. 1–269.

Dromart, G., Gaillard, C., Jansa, L.F., 1994. Deep-Marine Microbial Structures in the Upper Jurassic of Western Tethys, in: Bertrand-Sarfati, J., Monty, C. (Eds.), Phanerozoic Stromatolites II. Springer Netherlands, Dordrecht, pp. 295–318. https://doi.org/10.1007/978-94-011-1124-9_12

Dunham, R.J., 1962. Classification of carbonate rocks according to depositional texture. In: Ham, W.E. (Ed.), Classification of Carbonate Rocks. American Association of Petroleum Geologists Memoir vol. 1, pp. 108–121.

Dupraz, C., Strasser, A., 1999. Microbialites and micro-encrusters in shallow coral bioherms (Middle to Late Oxfordian, Swiss Jura mountains). Facies 40, 101–129. https://doi.org/10.1007/BF02537471

Dupraz, C., Strasser, A., 2002. Nutritional modes in coral-microbialite reefs (Jurassic, Oxfordian, Switzerland): Evolution of trophic structure as a response to environmental change. Palaios 17, 449–471. https://doi.org/10.1669/0883-1351

El-sabbagh, A.M., El-hedeny, M.M., Mansour, A.S., 2017. Paleoecology and Paleoenvironment of the Middle – Upper Jurassic sedimentary succession, central Saudi Arabia. Proceedings of the Geologists' Association 128, 340–359. https://doi.org/10.1016/j.pgeola.2017.02.001

Embry, A.F., Klovan, J.E., 1971. A Late Devonian reef tract on northeastern Banks Island, NWT. Bulletin of Canadian Petroleum Geology 19, 730–781. https://doi.org/10.5072/PRISM/22817

Flügel, E., 2004. Microfacies of Carbonate Rocks: Analysis, Interpretation and Application. 976 pp. Springer-Verlag, Berlin Heidelberg. https://doi.org/10.1007/978-3-642-03796-2

Guo, L., Vincent, S.J., Lavrishchev, V., 2011. Upper Jurassic Reefs from the Russian Western Caucasus: Implications for the Eastern Black Sea. Turkish Journal of Earth Sciences 20, 629–653. https://doi.org/10.3906/yer-1012-5

Hallock, P., 2015. Changing influences between life and limestones in earth history. In: Birkeland, C. (Ed.), Coral Reefs in the Anthropocene. Springer, Dordrecht, pp. 17–42. http://dx.doi.org/10.1007/978-94-017-7249-5.

Hallock, P., 1987. Fluctuations in the trophic resource continuum: a factor in global diversity cycles?. Paleoceanography and Paleoclimatology 2, 457-471.

Hallock, P., 2005. Global change and modern coral reefs: new opportunities to understand shallow-water carbonate depositional processes. Sedimentary Geology. 175, 19–33. http://dx.doi. org/10.1016/j.sedgeo.2004.12.027

Haq, B.U., 2018. Jurassic Sea-Level Variations: A Reappraisal. GSA Today 4–10. https://doi.org/10.1130/GSATG359A.1

Hoffmann, M., Kołodziej, B., Skupien, P., 2017. Microencruster-microbial framework and synsedimentary cements in the Štramberk Limestone (Carpathians, Czech Republic): Insights into reef zonation. Annales Societatis Geologorum Poloniae 87, 325–347. https://doi.org/10.14241/asgp.2017.018

Holz, M., 2015. Mesozoic paleogeography and paleoclimates - A discussion of the diverse greenhouse and hothouse conditions of an alien world. Journal of South American Earth Sciences 61, 91–107. https://doi.org/10.1016/j.jsames.2015.01.001

Immenhauser, A., 2009. Estimating palaeo-water depth from the physical rock record. Earth-Science Reviews 96, 107–139. https://doi.org/10.1016/j.earscirev.2009.06.003

Insalaco, E., 1999. Facies and Palaeoecology of Upper Jurassic (Middle Oxfordian) Coral Reefs in England. Facies 40, 81–99. https://doi.org/10.1007/BF02537470

Insalaco, E., 1996. Upper Jurassic microsolenid biostromes of northern and central of northern and central. Europe: Facies and depositional environment. Palaeogeography, Palaeoclimatology, Palaeoecology. 121, 169-194.

Insalaco, E., Hallam, A., Rosen, B., 1997. Oxfordian (Upper Jurassic) coral reefs in Western Europe: reef types and conceptual depositional model. Sedimentology 44, 707–734. https://doi.org/10.1046/j.1365-3091.1997.d01-44.x

Jakubowicz, M., Król, J., Zapalski, M.K., Wrzołek, T., Wolniewicz, P., Berkowski, B., 2018. At the southern limits of the Devonian reef zone: Palaeoecology of the Aferdou el Mrakib reef (Givetian, eastern Anti-Atlas, Morocco). Geological Journal 1–29. https://doi.org/10.1002/gj.3152

James, N.P., Bourque, P.A., 1992. Reefs and mounds. In: Walker, R.G., James, N.P. (Eds.), Facies Models: Response to Sea Level Change. Geological Association of Canada, St. John's, Newfoundland, pp. 323–347.

Kano, A., Wang, W., Matsumoto, R., 2007. Facies and depositional environment of the uppermost Jurassic stromatoporoid biostromes in the Zagros Mountains of Iran. Gff 129, 107–112. https://doi.org/10.1080/11035890701292107

Kershaw, S., 1998. The applications of stromatoporoid palaeobiology in palaeoenvironmental analysis. Palaeontology 41, 3, 509–544.

Kershaw, S., Min, L., Yuan, W., 2013. Palaeozoic stromatoporoid futures: A discussion of their taxonomy, mineralogy and applications in palaeoecology and palaeoenvironmental analysis. Journal of Palaeogeography 2, 163–182. https://doi.org/10.3724/SP.J.1261.2013.00024

Kershaw, S., Mõtus, M., 2016. Palaeoecology of corals and stromatoporoids in a late Silurian biostrome in Estonia. Acta Palaeontologica Polonica 61, 33–50. https://doi.org/10.4202/app.00094.2014

Kiessling, W., 2002. Secular variations in the Phanerozoic reef ecosystem. In: Kiessling, W., Flü gel, E., Golonka, J. (Eds.), Phanerozoic Reef Patterns, Society of Economic Paleontologists and Mineralogists. Special Publication 72, pp. 625 – 690. Tulsa

Kiessling, W., 2009. Geologic and Biologic Controls on the Evolution of Reefs. Annual Review of Ecology, Evolution, and Systematics 40, 173–192. https://doi.org/10.1146/annurev.ecolsys.110308.120251

Krajewski, M., Olchowy, P., Felisiak, I., 2016. Late Jurassic facies architecture of the Złoczew Graben: implications for evolution of the tectonic-controlled northern peri-Tethyan shelf (Upper

Oxfordian–Lower Kimmeridgian, Poland). Facies 62, 1–19. https://doi.org/10.1007/s10347-015-0455-3

Lamb, K.G., 2014. Internal Wave Breaking and Dissipation Mechanisms on the Continental Slope/Shelf. Annual Review of Fluid Mechanics 46, 231–254. https://doi.org/10.1146/annurev-fluid-011212-140701

Lathuilière, B., Gaillard, C., Habrant, N., Bodeur, Y., Boullier, A., Enay, R., Hanzo, M., Marchand, D., Thierry, J., Werner, W., 2005. Coral zonation of an Oxfordian reef tract in the northern French Jura. Facies 50, 545–559. https://doi.org/10.1007/s10347-004-0035-4

Leichter, J.J., Stewart, H.L., Miller, S.L., 2003. Episodic nutrient transport of Florida coral reefs. Limnology and Oceanography 48,1394–1407.

Leinfelder, R.R., 1993. Upper Jurassic reef types and controlling factors. A preliminary report. Profil 5, 1–45.

Leinfelder, R.R., Werner, W., Nose, M., Schmid, D.U., Krautter, M., Laternser Tokacs, M., Hartmann, D., 1996. Paleoecology, growth parameters and dynamics of coral, sponge and microbolite reefs from the Late Jurassic. Göttinger Arbeiten zur Geologie und Paläontologie 2, 227–248.

Leinfelder, R.R., Schlagintweit, F., Werner, W., Ebli, O., Nose, M., Schmid, D.U., Hughes, G.W., 2005. Significance of stromatoporoids in Jurassic reefs and carbonate platforms - Concepts and implications. Facies 51, 287–325. https://doi.org/10.1007/s10347-005-0055-8

Leinfelder, R.R., Schmid, D.U., Nose, M., Werner, W., 2002. Jurassic reef patterns. The expression of a changing globe. In: Kiessling, W., Flügel, E., Golonka, J. (Eds.), Phanerozoic Reef Patterns: SEPM Special Publication 72, 465–520.

Luperto Sinni, E., Masse, J.P., 1994). Precisazioni micropaleontologiche sulle formazioni di piattaforma carbonatica del Giurassico superiore e del Cretaceo basale del massiccio del Gargano (Italia Meridionale) e implicazioni stratigrafiche. Paleopelagos 4, 243-266.

Martin-Garin, B., Lathuilière, B., Geister, J., 2012. The shifting biogeography of reef corals during the Oxfordian (Late Jurassic). A climatic control?. Palaeogeography, Palaeoclimatology, Palaeoecology 365–366, 136–153. https://doi.org/10.1016/j.palaeo.2012.09.022

Matyszkiewicz, J., Kochman, A., Duś, A., 2012. Influence of local sedimentary conditions on development of microbialites in the Oxfordian carbonate buildups from the southern part of the Kraków–Częstochowa Upland (South Poland). Sedimentary Geology 263–264, 109–132. https://doi.org/10.1016/j.sedgeo.2011.08.005

Michel, J., Borgomano, J., Reijmer, J.J.G., 2018. Heterozoan carbonates: When, where and why? A synthesis on parameters controlling carbonate production and occurrences. Earth-Science Reviews 182, 50–67. https://doi.org/10.1016/j.earscirev.2018.05.003

Morsilli, M., Bosellini, A., 1997. Carbonate facies zonation of the Upper Jurassic–Lower Cretaceous Apulia platform margin (Gargano Promontory, southern Italy). Rivista Italiana Paleontologia Stratigrafica 103, 193–206.

Morsilli, M., 1998. Stratigrafia e sedimentologia del margine della piattaforma Apula nel Gargano (Giurassico superiore - Cretaceo inferiore). PhD thesis. University of Bologna. 222 pp.

Morsilli, M., 2011. Introduzione alla geologia del Gargano, in M. Tarantini and A. Galiberti, eds., Le Miniere Di Selce Del Gargano, VI-III Millennio a.C. Alle Origini Della Storia Mineraria Europea: Florence, Italy, All'Insegna del Giglio, 17–27.

Morsilli, M., Bosellini, F.R., Pomar, L., Hallock, P., Aurell, M., Papazzoni, C.A., 2012. Mesophotic coral buildups in a prodelta setting (Late Eocene, southern Pyrenees, Spain): A mixed carbonate-siliciclastic system. Sedimentology 59, 766–794. https://doi.org/10.1111/j.1365-3091.2011.01275.x

Morsilli, M., Hairabian, A., Borgomano, J., Nardon, S., Adams, E., Gartner, G.B., 2017. The Apulia Carbonate Platform—Gargano Promontory, Italy (Upper Jurassic–Eocene). American Association of Petroleum Geologists Bulletin 101, 523–531. https://doi.org/10.1306/011817DIG17031

Munk, W., 1981. Internal waves and small-scale processes. In: Warren, B.A., Wunsch, C. (Eds.), Evolution of Physical Oceanography. MIT Press, Cambridge, pp. 264–291.

Mutti, M., Hallock, P., 2003. Carbonate systems along nutrient and temperature gradients: some sedimentological and geochemical constraints. International Journal of Earth Sciences 92, 465–475.

Olivier, N., Carpentier, C., Martin-Garin, B., Lathuilière, B., Gaillard, C., Ferry, S., Hantzpergue, P., Geister, J., 2004. Coral-microbialite reefs in pure carbonate versus mixed carbonate-siliciclastic depositional environments: The example of the Pagny-sur-Meuse section (Upper Jurassic, northeastern France). Facies 50, 229–255. https://doi.org/10.1007/s10347-004-0018-5

Olivier, N., Colombié, C., Pittet, B., Lathuilière, B., 2011. Microbial carbonates and corals on the marginal French Jura platform (Late Oxfordian, Molinges section). Facies 57, 469–492. https://doi.org/10.1007/s10347-010-0246-9

Olivier, N., Hantzpergue, P., Gaillard, C., Pittet, B., Leinfelder, R.R., Schmid, D.U., Werner, W., 2003. Microbialite morphology, structure and growth: a model of the Upper Jurassic reefs of the Chay Peninsula (western France). Palaeogeography, Palaeoclimatology, Palaeoecology 193, 383–404.

Olivier, N., Martin-Garin, B., Colombié, C., Cornée, J.J., Giraud, F., Schnyder, J., Kabbachi, B., Ezaidi, K., 2012. Ecological succession evidence in an Upper Jurassic coral reef system (Izwarn section, High Atlas, Morocco). Geobios 45, 555–572. https://doi.org/10.1016/j.geobios.2012.05.002

Olivier, N., Pittet, B., Gaillard, C., Hantzpergue, P., 2007. High-frequency palaeoenvironmental fluctuations recorded in Jurassic coral- and sponge-microbialite bioconstructions. Comptes Rendus Palevol 6, 21–36. https://doi.org/10.1016/j.crpv.2006.07.005

Olivier, N., Pittet, B., Werner, W., Hantzpergue, P., Gaillard, C., 2008. Facies distribution and coral-microbialite reef development on a low-energy carbonate ramp (Chay Peninsula, Kimmeridgian, western France). Sedimentary Geology 205, 14–33. https://doi.org/10.1016/j.sedgeo.2007.12.011

Olóriz, F., Reolid, M., Rodríguez-Tovar, F.J., 2003. A Late Jurassic carbonate ramp colonized by sponges and benthic microbial communities (External Prebetic, Southern Spain). Palaios 18, 528–545.

Pandey, D.K., Fürsich, F.T., 2003. Jurassic corals of east-central Iran. Beringeria 32, 1–138.

Pavan, G., Pirini, C., 1966. Stratigrafia del Foglio 157 ‘‘Monte S. Angelo’’. Bollettino del Servizio Geologico Italiano 86, 123–189.

Picotti, V., Cobianchi, M., 2017. Jurassic stratigraphy of the Belluno Basin and Friuli Platform: a perspective on far-field compression in the Adria passive margin. Swiss Journal of Geosciences 110, 833–850. https://doi.org/10.1007/s00015-017-0280-5

Pomar, L., 2001. Types of carbonate platforms: A genetic approach. Basin Research 13, 313–334. https://doi.org/10.1046/j.0950-091X.2001.00152.x

Pomar, L., Baceta, J.I., Hallock, P., Mateu-Vicens, G., Basso, D., 2017. Reef building and carbonate production modes in the west-central Tethys during the Cenozoic. Marine and Petroleum Geology 83, 261–304. https://doi.org/10.1016/j.marpetgeo.2017.03.015

Pomar, L., Hallock, P., 2008. Carbonate factories: A conundrum in sedimentary geology. Earth-Science Reviews 87, 134–169. https://doi.org/10.1016/j.earscirev.2007.12.002

Pomar, L., Morsilli, M., Hallock, P., Bádenas, B., 2012. Internal waves, an under-explored source of turbulence events in the sedimentary record. Earth-Science Reviews 111, 56–81. https://doi.org/10.1016/j.earscirev.2011.12.005

Reolid, M., Gaillard, C., Lathuilière, B., 2007. Microfacies, microtaphonomic traits and foraminiferal assemblages from Upper Jurassic oolitic-coral limestones: Stratigraphic fluctuations in a shallowing-upward sequence (French Jura, Middle Oxfordian). Facies 53, 553–574. https://doi.org/10.1007/s10347-007-0121-5

Reolid, M., Gaillard, C., Olóriz, F., Rodríguez-Tovar, F.J., 2005. Microbial encrustations from the Middle Oxfordian-earliest Kimmeridgian lithofacies in the Prebetic Zone (Betic Cordillera, southern Spain): Characterization, distribution and controlling factors. Facies 50, 529–543. https://doi.org/10.1007/s10347-004-0030-9

Riding, R., 2002. Structure and composition of organic reefs and carbonate mud mounds: Concepts and categories. Earth-Science Reviews 58, 163–231. https://doi.org/10.1016/S0012-8252(01)00089-7

Rosales, I., Pomar, L., Al-Awwad, S.F., 2018. Microfacies, diagenesis and oil emplacement of the Upper Jurassic Arab-D carbonate reservoir in an oil field in central Saudi Arabia (Khurais Complex). Marine and Petroleum Geology 96, 551–576. https://doi.org/10.1016/j.marpetgeo.2018.05.010

Rusciadelli, G., Ricci, C., Lathuilière, B., 2011. The Ellipsactinia Limestones of the Marsica area (Central Apennines): A reference zonation model for Upper Jurassic Intra-Tethys reef complexes. Sedimentary Geology 233, 69–87. https://doi.org/10.1016/j.sedgeo.2010.10.011

Russo, A., Morsilli, M., 2007. New insight on architecture and microstructure of *Ellipsactinia* and *Sphaeractinia* (demosponges) from the Gargano Promontory (southern Italy). Geologica Romana 40, 215–225.

San Miguel, G., Aurell, M., Bádenas, B., 2017. Occurrence of high-diversity metazoan- to microbial-dominated bioconstructions in a shallow Kimmeridgian carbonate ramp (Jabaloyas, Spain). Facies 63, 1–21. https://doi.org/10.1007/s10347-017-0493-0

Schlager, W., 2000. Sedimentation rates and growth potential of tropical, cool water and mud mound carbonate factories. In: Insalaco, E., Skelton, P.W., Palmer, T.J. (Eds.), Carbonate Platform Systems: Components and Interactions. Geological Society London, Special Publication., 178, pp. 217–227. http://dx.doi.org/10.1144/GSL.SP.2000.178.01.14.

Schlager, W., 2003. Benthic carbonate factories of the Phanerozoic. International Journal of Earth Sciences. (Geol. Rundsch.) 92, 445–464. http://dx.doi.org/10.1007/s00531-003-0327-x.

Schlagintweit, F., Gawlick, H.J., 2008. The occurrence and role of microencruster frameworks in Late Jurassic to Early Cretaceous platform margin deposits of the Northern Calcareous Alps (Austria). Facies 54, 207–231.

Schlagintweit, F., Gawlick, H.J., Missoni, S., Lein, R., 2005. The reefal facies of the Upper Jurassic Plassen carbonate platform at Mt. Jainzen (Northern Calcareous Alps, Austria). Schriftenreihe der Deutschen Gesellschaft für Geowissenschaften 38, 130–131.

Schmid, D.U., 1996. Marine Mikrobolithe und Mikroinkrustierer aus dem Oberjura. Profil 9, 101–251.

Shanmugam, G., 2013. Modern internal waves and internal tides along oceanic pycnoclines: Challenges and implications for ancient deep-marine baroclinic sands. American Association of Petroleum Geologists Bulletin 97, 799. https://doi.org/10.1306/10171212101

Strasser, A., Pittet, B., Hug, W., 2015. Palaeogeography of a shallow carbonate platform: The case of the Middle to Late Oxfordian in the Swiss Jura Mountains. Journal of Palaeogeography 4, 251–268. https://doi.org/10.1016/j.jop.2015.08.005

Strasser, A., Védrine, S., 2009. Controls on facies mosaics of carbonate platforms: a case study from the Oxfordian of the Swiss Jura. International Association of Sedimentologists, Special Publication 41, 199–214. https://doi.org/10.1002/9781444312065.ch13

Turnšek, D., Buser, S., Ogorolec, B., 1981. An upper Jurassic reef complex from Slovenia, Yugoslavia. In: Toomey, D.F. (Ed.), European Fossil Reef Models: SEPM Special Publication 30, 361–369.

Wilson, M.E.J., Vecsei, A., 2005. The apparent paradox of abundant foramol facies in low latitudes: their environmental significance and effect on platform development. Earth-Science Reviews 69, 133–168.

Wood, R., 1999. Reef Evolution. Oxford University Press, Oxford, 414 pp.

Woodson, C.B., 2018. The Fate and Impact of Internal Waves in Nearshore Ecosystems. Annual Review of Marine Science 10, 421-441.

Figure captions

Fig. 1.

Schematic paleogeographic map of Tethys during the Late Jurassic (modified from Dercourt et al., 2000), showing the distribution of different type of reefs. 1- Jura Platform, 2- France Lorraine, 3- Switzerland and northern Germany, 4- England (Yorkshire), 5- France Burgundy, 6- Pagny-sur-Meuse, 7-8- Iberian basin, 9- La Rochelle platform, 10- Zagros basin, 11- Khurais basin, 12- Dinaric carbonate platform? 13- Apulia carbonate platform (this study, black arrow), 14- Sicily, 15- Apennines carbonate platform, 16- Friuli. The data extracted from various researches (Turnšek et al., 1981; Morsilli and Bosellini, 1997; Insalaco et al., 1997, 1999; Olóriz et al., 2003; Lathuilière et al., 2005; Leinfelder et al., 2005; Kano et al., 2007; Olivier et al., 2008; Rusciadelli et al., 2011; Al-Awwad and Pomar, 2015; Basilone and Sulli, 2016a; San Miguel et al., 2017).

Fig. 2.

A) Schematic palaeogeographic map showing the location of studied area (Gargano Promontory) along the platform margin of ACP (modified from Dercourt et al., 2000). (B)

Stratigraphic framework of the Gargano area during the Late Jurassic and Early Cretaceous succession. The studied interval belongs to Monte Sacro Limestones (red square) (modified from Morsilli, 2016). (C) Simplified geological map of the Gargano Promontory showing different facies zones and study areas of this paper (modified after Morsilli, 2011). Coordinates: top left corner (41°589 6.340 N; 15°179 26.930 E); bottom right corner (41°329 57.660 N; 16°129

25.560 E). Study areas: 1- Torre Mileto 2- Monte di Mezzo 3- Masseria Prencipe. The external margin deposits are representing by Monte Sacro Limestones.

Fig. 3.

(A) Google map showing the position of studied lithofacies (LF1, LF2, LF3) and one stratigraphic log (section A) along the road of Monte di Mezzo section. LF1 is the more abundant lithofacies followed by LF2 and LF1. (B). The stratigraphic log (section A) of stromatoporoid-rich facies showing the distribution of subfacies (LF1-S1 and LF2-2) and in a vertical position. The *in-situ* stromatoporoids (LF1-S1) are more concentrated towards the top of section when the energy is low. (C). Figure shows the distribution of stromatoporoids on the surface of outcrop in Monte di Mezzo. The organization of biotic components show a cluster reef fabric (*sensu* Riding, 2002) (D). The figure indicates the organization of studied subfacies (LF1-S1 and LF2-2) on the surface of outcrop.

Fig. 4.

Field observations of outcrops with their sketches show (A) the distribution of *in-situ* corals and stromatoporoids (*Ellipsactinia* sp.and *Sphaeractinia* sp.) in LF2-S2 subfacies in Monte di Mezzo section. (B). The LF2-S2 occur in cm- thick massive limestone and represented by tabular form stromatoporoids associated with *in-situ* coral colonies (Masseria Prencipe section). (C). The LF3 is characterized by stromatolite-like structure followed by stromatoporoids (*Ellipsactinia* sp.and *Sphaeractinia* sp.) on the top (Monte di Mezzo section).

Fig. 5.

(A) Pie charts showing the distribution of lithofacies LF1, LF2, LF3 in studied area (in percentage). The Stromatoporoid-rich facies (LF1) is the main lithofacies followed by LF2 and LF3. (B) The chart shows the percentage of subfacies LF1-S1 and LF1-S2 in stromatoporoid-rich facies. The subfacies LF1-S2 is more abundant compare with LF1-S2, showing the high percentage of debris contributed in formation of stromatoporoid-rich facies in MSL.

Fig. 6.

Stromatoporoid-rich lithofacies (LF1). (A), (B) distribution of subfacies LF1-S1 and LF1-S2 on the surface of outcrop with their sharp boundaries (Torre Mileto section) and (C) Monte di Mezzo section. (D). Thin section image shows the stromatoporoid (stro) surrounded by a wackestone (W) matrix in (LF1-S1). (E) The image shows the mm to cm-sized intraclasts and bioclasts distributed in a grainstone matrix (LF1-S2). The micro-encrusters are developed around the coral fragments and represented mostly by *Tubiphytes* sp.(G) The LF1-S2 in this image is characterized by mm to cm-sized intraclasts and bioclasts distributed in a packstone (P) matrix.

Fig. 7.

Stromatoporoid-rich lithofacies (LF1) (continue). (A) Figure shows the bulbous growth form of an *in-situ Ellipsactinia* sp. (B) *Sphaeractinia* sp. stromatoporoid shows an *in-situ* columnar growth shape. Note the lamellae are thinner than inter-lamellar spaces or show the same size compare with *Ellipsactinia* sp. (Figs. 7A, C). (C) An *Ellipsactinia* sp. shows an *in-situ* robust dendroid form. (D) Thin section image of *Ellipsactinia* sp. with lamellae are thicker than inter-lamellar space. (E) Thin section image shows *Tubiphytes* sp. (red arrows). growing in association with stromatoporoids.

Fig. 8.

Stromatoporoid- coral facies (LF2) (LF2-S1). (A) Photo shows the position and size of coral colonies in outcrop. (B) The coral shows a roboust branching. (C), (D), (F**)** The field photos of coral colonies show growth form of *in-situ* colonies. Note that the corals show branching growth form with delicate branches that positioned in close to each other.

Fig.9.

(A) Thin section photo of LF2-S1 shows a packstone matrix rich in peloids and *Tubiphytes* sp . nodules. (B) Thin section photo of LF2-S1 subfacies showing h a wackestone matrix with *Saccocoma* sp. (C) A close view of *Saccocoma* sp. (white arrow) distributed in wackestone matrix of LF2-S1. (D) A photomicrograph shows a *Tubiphytes* sp. in growth position (red arrow) associated with other fragment of *Tubiphytes* sp.

Fig.10.

Stromatoporoid- coral facies (LF2) (LF2-S2). (A) Photo shows a tabular stromatoporoid colony developed in Masseria Prencipe area. (B) Image shows the co-occurrence of *in-situ* phaceloid form coral colonies associated with tabular stromatoporoid (stro). (C) Thin section photo of tabular stromatoporoids surrounded by a wackestone (W) matrix rich in radiolarians.

Fig.11.

Stromatoporoid- microbial facies (LF3). (A) Field photo shows the distribution of stromatoporoids, spongy- like organisms and echinoids accompanied with stromatolite- like structures. (B**)** A close view of stromatolite- like structures. (C) Thin section photo shows the in-growth form of stromatoporoids (sto, white arrow) (*Cylicopsis* sp.?) surrounded by a wackestone to packstone matrix. (D) Thin section photo of stromatolite-like structures shows the alternation of dark and clear laminae of stromatolites (white arrows). (E) photomicrograph shows a microbial mat-like character (white arrows) of dark laminations alternating with clear laminae (Fig. 11D).

Fig. 12.

Schematic depositional model of the Gargano margin during the Late Jurassic-Early Cretaceous (modified after Morsilli and Bosellini, 1997). The model shows the facies belts from inner platform, margin, slope to base-of-slope to basin.

Fig. 13.

Schematic cross section of external marginal facies of the Monte Sacro Limestones in Gargano area. Lateral distribution of lithofacies, internal sediment textures, and main carbonate particles of various lithofacies are shown.

Fig. 14.

A general schematic diagram showing the major control factors on the growth, dominated biota groups and distribution of Upper Jurassic reefs of northern Tethys on a carbonate platform (modified from Leinfelder et al., 2002) and stromatoporoid-rich buildups in Apulia Carbonate Platform (ACP). The information used in this figure are extracted from Insalaco, 1996; Dupraz and Strasser, 2002; Olóriz et al., 2003; Olivier et al., 2007, 2011). (SSW: surface storm waves, IW: internal waves, FWWB: fair weather wave base, SWB: storm wave base, S.L: sea level)

Fig. 15.

Stromatoporoid-rich facies and stromatoporoid- coral facies developed in the mesophotic zone, below the surface storm wave action; in this environments, episodic strong turbulence events hitting the buildups provided the energy to produce intraclast- bioclast rudstone to floatstone debris between bioconstructors.

Fig. 16.

Figure illustrating the different growth stages of stromatoporoid-rich facies (LF1) in Monte Sacro Limestone. (A) the stromatoporoids developed in a quiet environment and mud-dominated substrates (LF1-S1). (B) Internal waves provide a high energy turbulence event hitting the buildups and result in the production of debris rich facies in buildups (LF1-S2). Apart from hydrodynamic energy, Internal waves can also provide nutrients to the buildups. (C) The stromatoporoids can regenerate again (LF1-S1) due to nutrient availability provided by internal waves in a calm environment before hitting by episodic high-energy events again.

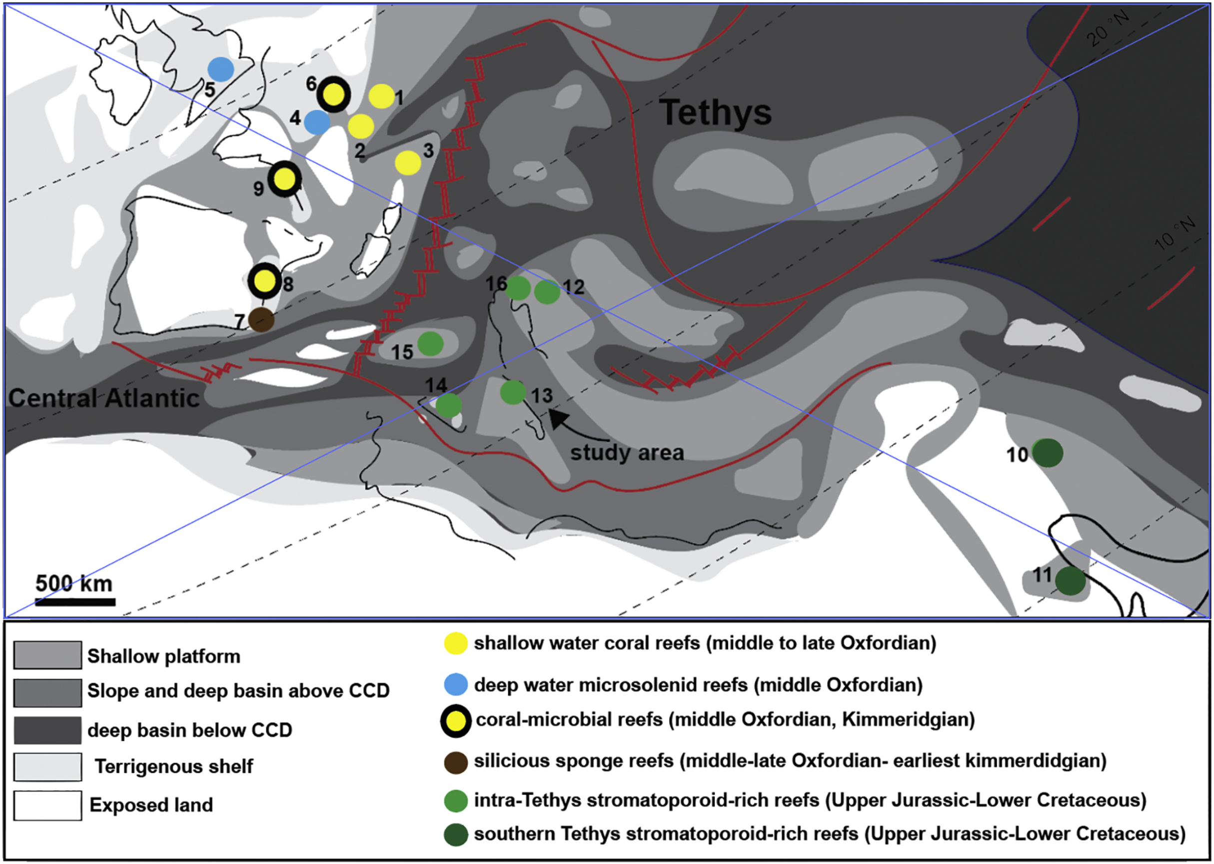

Tethys
Central Atlantic
study area
500 km
20 °N
10 °N
1
2
3
4
5
6
7
8
9
10
11
12
13
14
15
16
Shallow platform
Slope and deep basin above CCD
deep basin below CCD
Terrigenous shelf
Exposed land
shallow water coral reefs (middle to late Oxfordian)
deep water microsolenid reefs (middle Oxfordian)
coral-microbial reefs (middle Oxfordian, Kimmeridgian)
silicious sponge reefs (middle-late Oxfordian- earliest kimmerdidgian)
intra-Tethys stromatoporoid-rich reefs (Upper Jurassic-Lower Cretaceous)
southern Tethys stromatoporoid-rich reefs (Upper Jurassic-Lower Cretaceous)

Figure 1

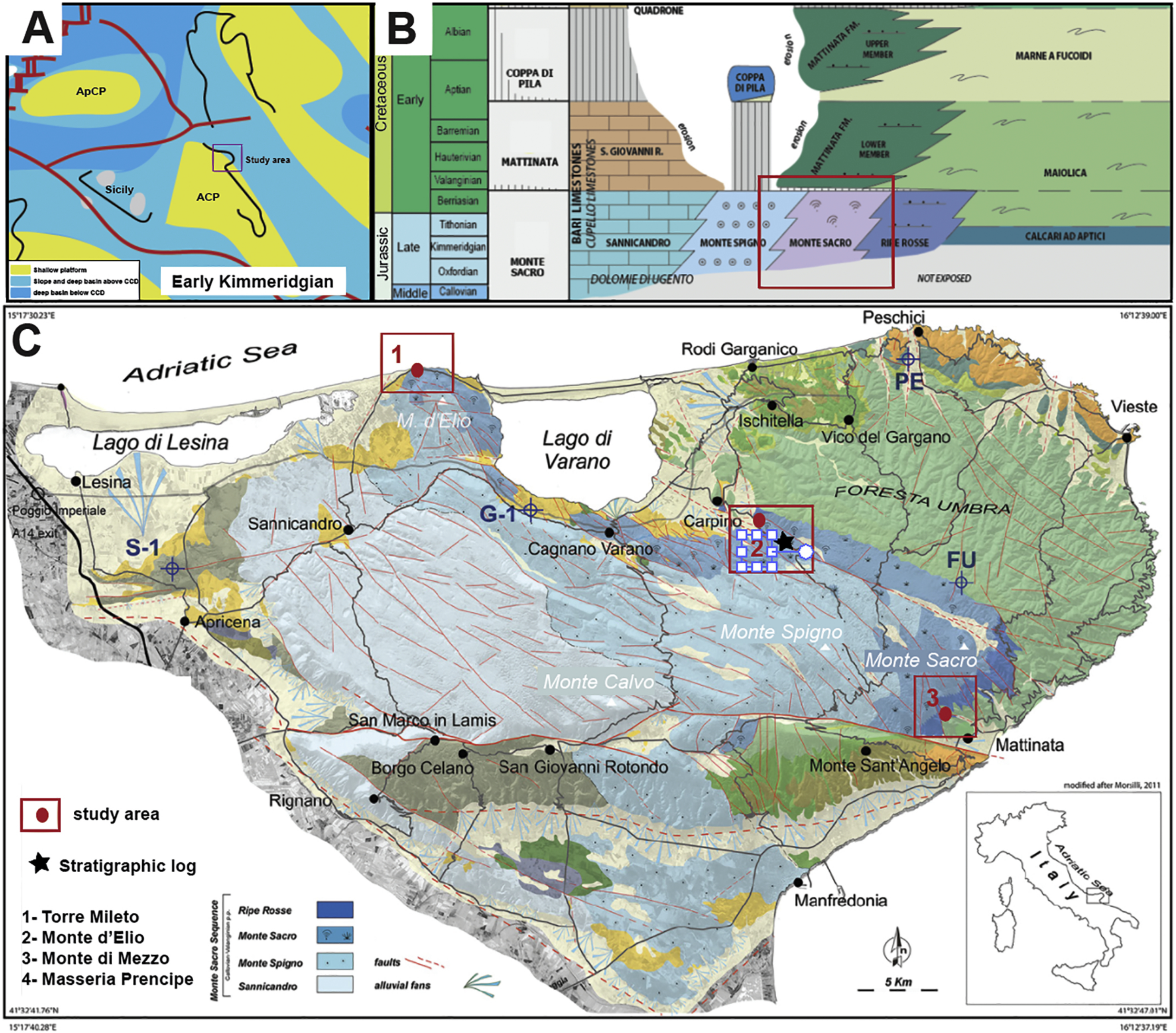
A
ApCP
ACP
Sicily
Study area
Shallow platform
Slope and deep basin above CCD
deep basin below CCD
Early Kimmeridgian
B
Cretaceous
Early
Albian
Aptian
Barremian
Hauterivian
Valanginian
Berriasian
Jurassic
Late
Middle
Tithonian
Kimmeridgian
Oxfordian
Callovian
COPPA DI PILA
MATTINATA
MONTE SACRO
QUADRONE
BARI LIMESTONES
CUPELLO LIMESTONES
S. GIOVANNI R.
SANNICANDRO
MONTE SPIGNO
MONTE SACRO
RIPE ROSSE
DOLOMIE DI UGENTO
NOT EXPOSED
erosion
COPPA DI PILA
MATTINATA FM. UPPER MEMBER
MATTINATA FM. LOWER MEMBER
MARNE A FUCOIDI
MAIOLICA
CALCARI AD APTICI
C
Adriatic Sea
Lago di Lesina
Lago di Varano
Lesina
Poggio Imperiale
A14 exit
S-1
G-1
PE
FU
M. d'Elio
Sannicandro
Cagnano Varano
Carpino
Rodi Garganico
Ischitella
Vico del Gargano
Peschici
Vieste
FORESTA UMBRA
Apricena
Monte Spigno
Monte Sacro
Monte Calvo
San Marco in Lamis
Borgo Celano
San Giovanni Rotondo
Rignano
Monte Sant'Angelo
Mattinata
Manfredonia
1
2
3
study area
Stratigraphic log
1- Torre Mileto
2- Monte d'Elio
3- Monte di Mezzo
4- Masseria Principe
Monte Sacro Sequence
Ripe Rosse
Monte Sacro
Monte Spigno
Sannicandro
faults
alluvial fans
5 Km
modified after Morsilli, 2011
Italy
Adriatic Sea
15°17'30.23"E
16°12'39.00"E
41°32'41.76"N
41°32'47.01"N
15°17'40.28"E
16°12'37.19"E

Figure 2

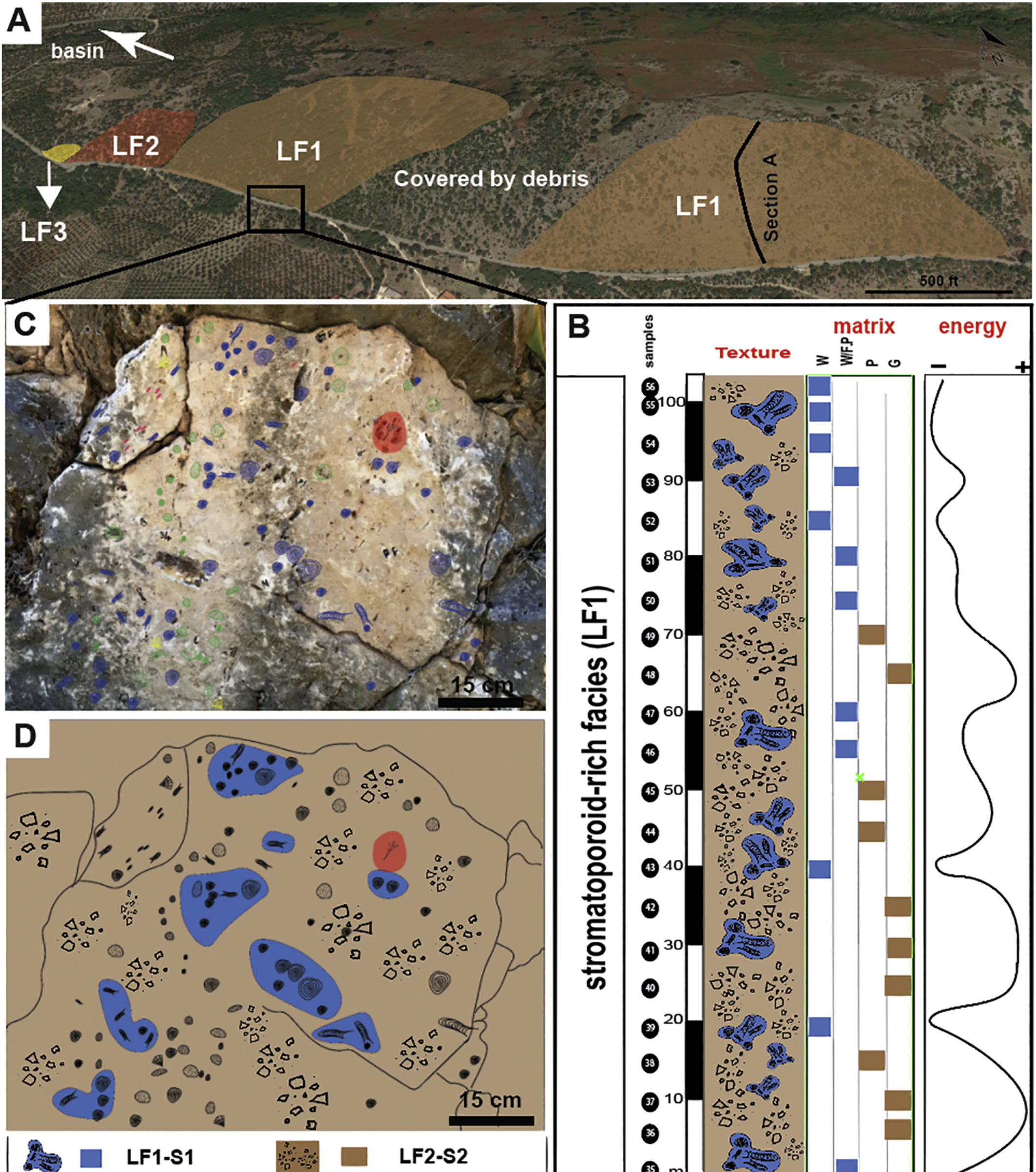

A
basin
LF2
LF1
LF3
Covered by debris
LF1
Section A
500 ft
C
15 cm
B
samples
Texture
matrix
W
W/FP
P
G
energy
-
+
stromatoporoid-rich facies (LF1)
100
90
80
70
60
50
40
30
20
10
m
56
55
54
53
52
51
50
49
48
47
46
45
44
43
42
41
40
39
38
37
36
35
D
15 cm
LF1-S1
LF2-S2

Figure 3

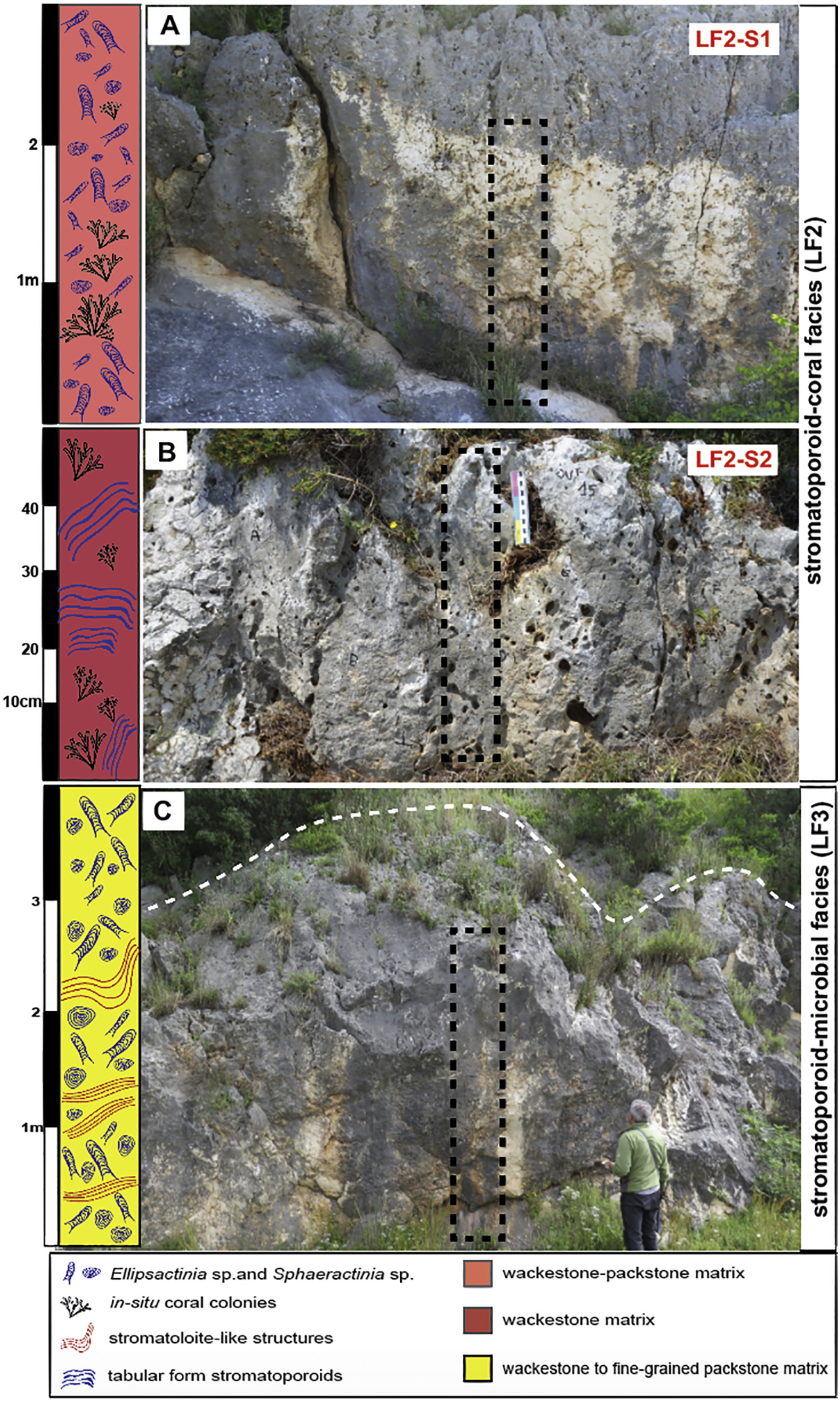
A
LF2-S1
B
LF2-S2
C
stromatoporoid-coral facies (LF2)
stromatoporoid-microbial facies (LF3)
2
1m
40
30
20
10cm
3
2
1m
Ellipsactinia sp.and Sphaeractinia sp.
in-situ coral colonies
stromatoloite-like structures
tabular form stromatoporoids
wackestone-packstone matrix
wackestone matrix
wackestone to fine-grained packstone matrix

Figure 4

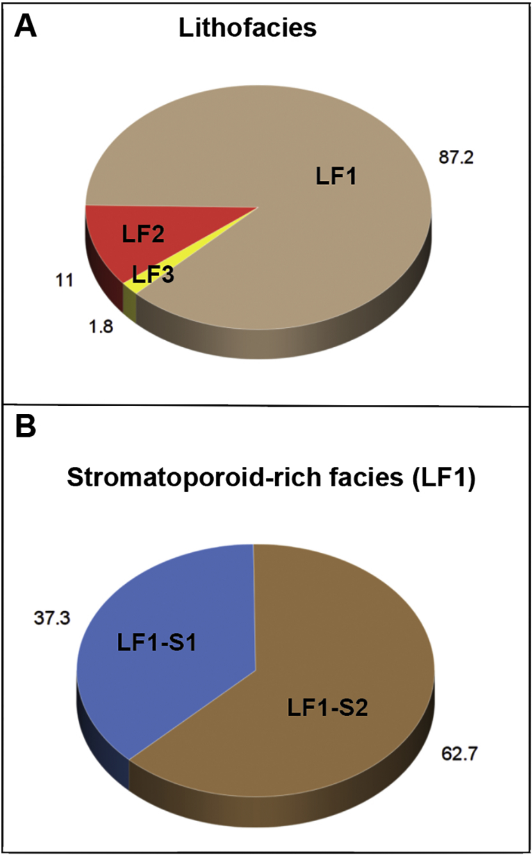
A
Lithofacies
LF1
87.2
LF2
11
LF3
1.8
B
Stromatoporoid-rich facies (LF1)
37.3
LF1-S1
LF1-S2
62.7

Figure 5

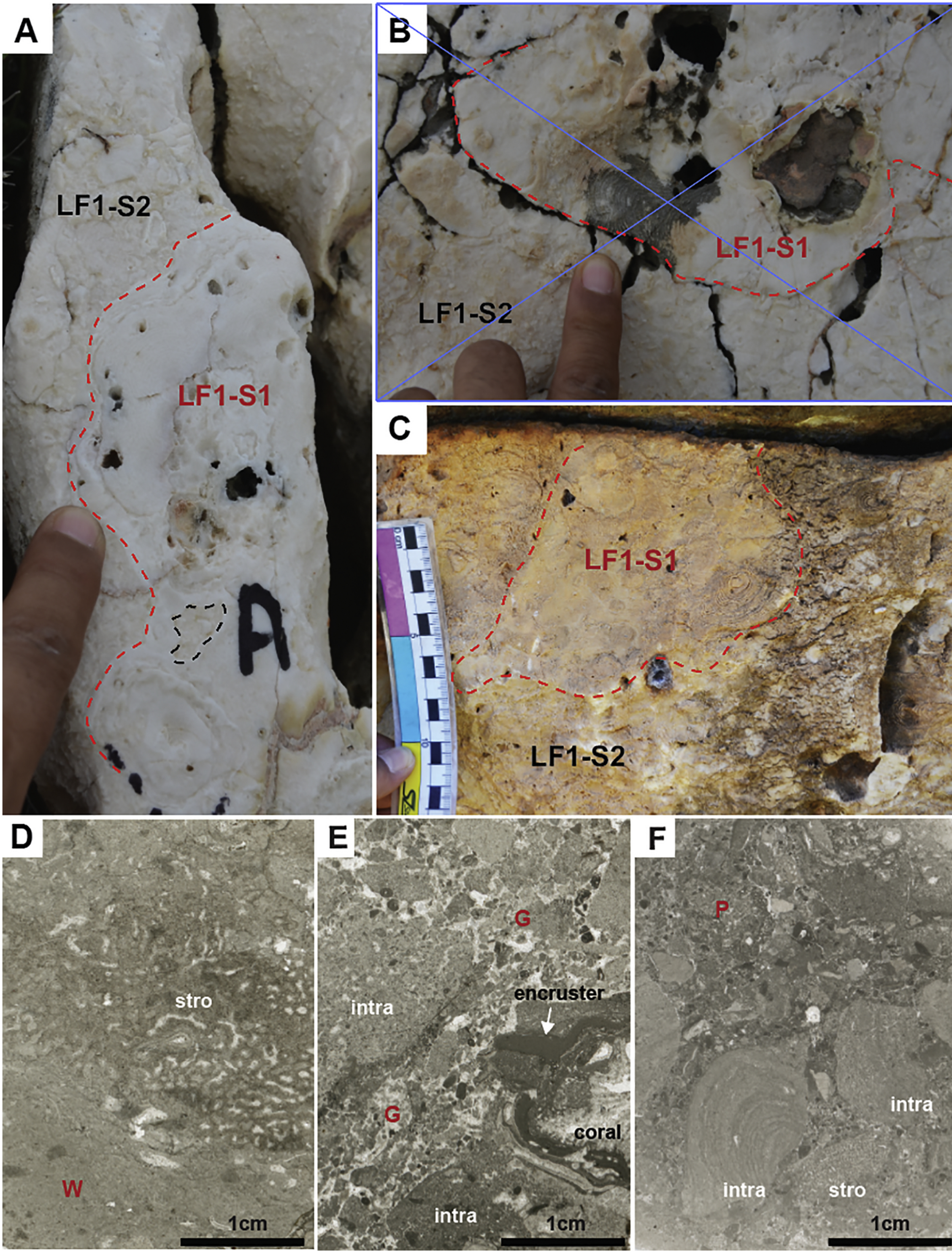
A
LF1-S2
LF1-S1
B
LF1-S1
LF1-S2
C
LF1-S1
LF1-S2
D
stro
W
1cm
E
G
intra
encruster
G
coral
intra
1cm
F
P
intra
intra
stro
1cm

Figure 6

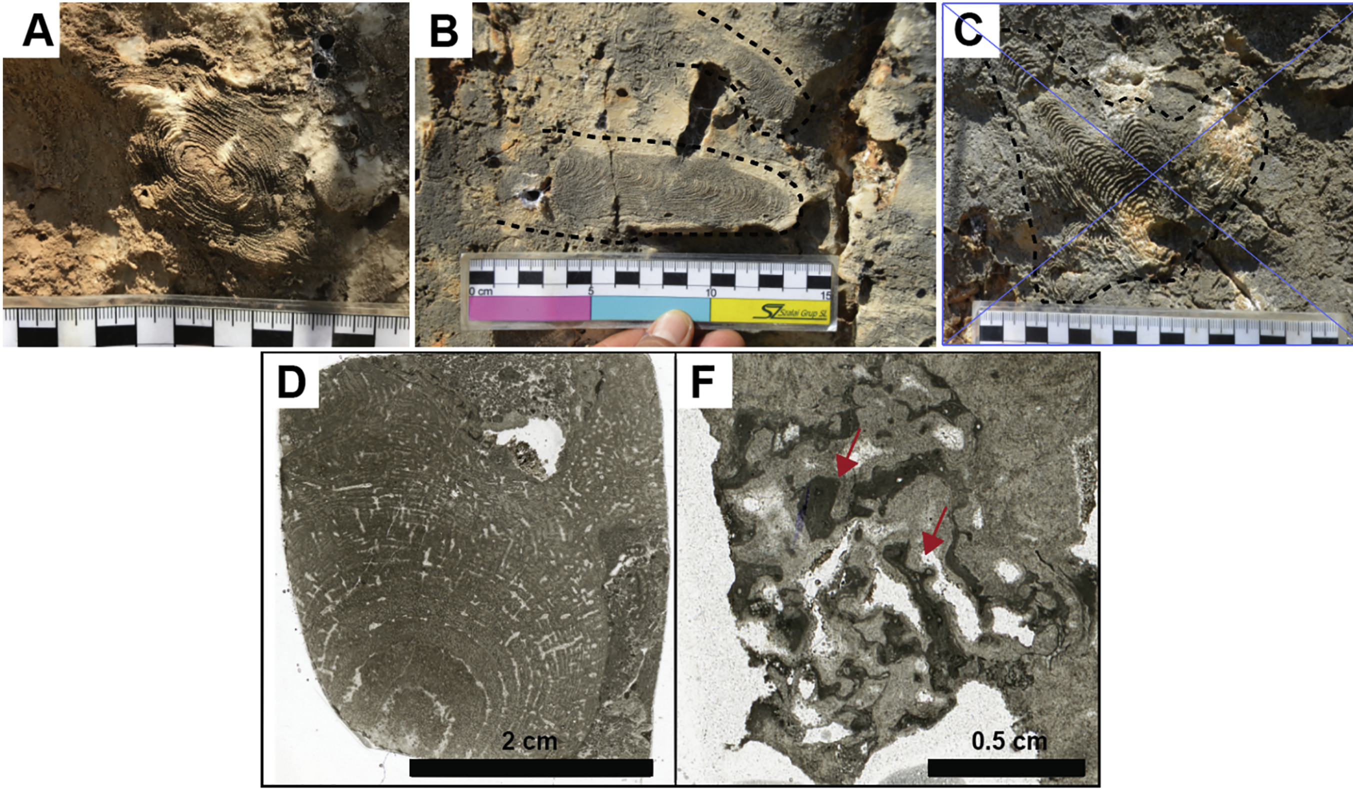

Figure 7

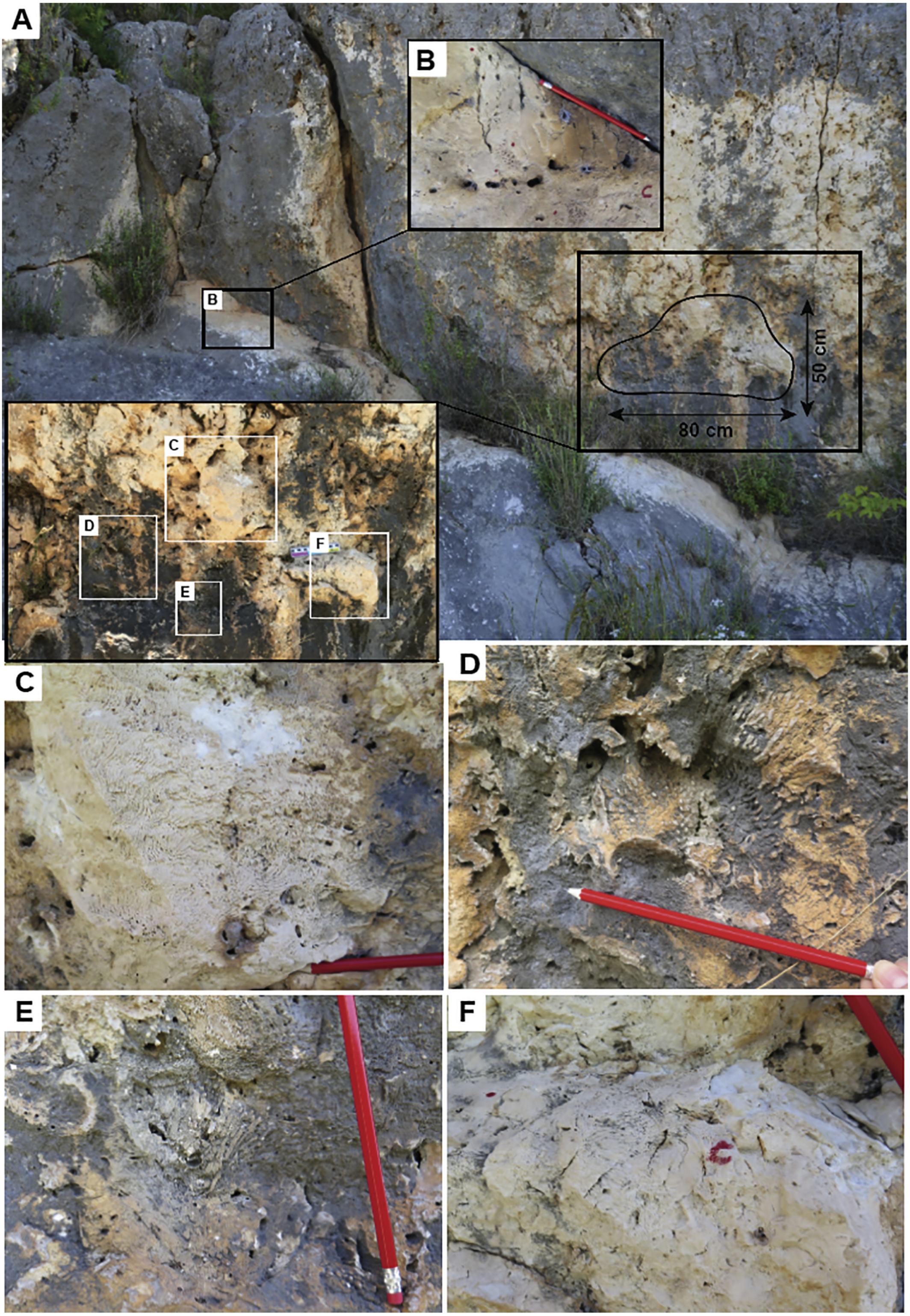

Figure 8

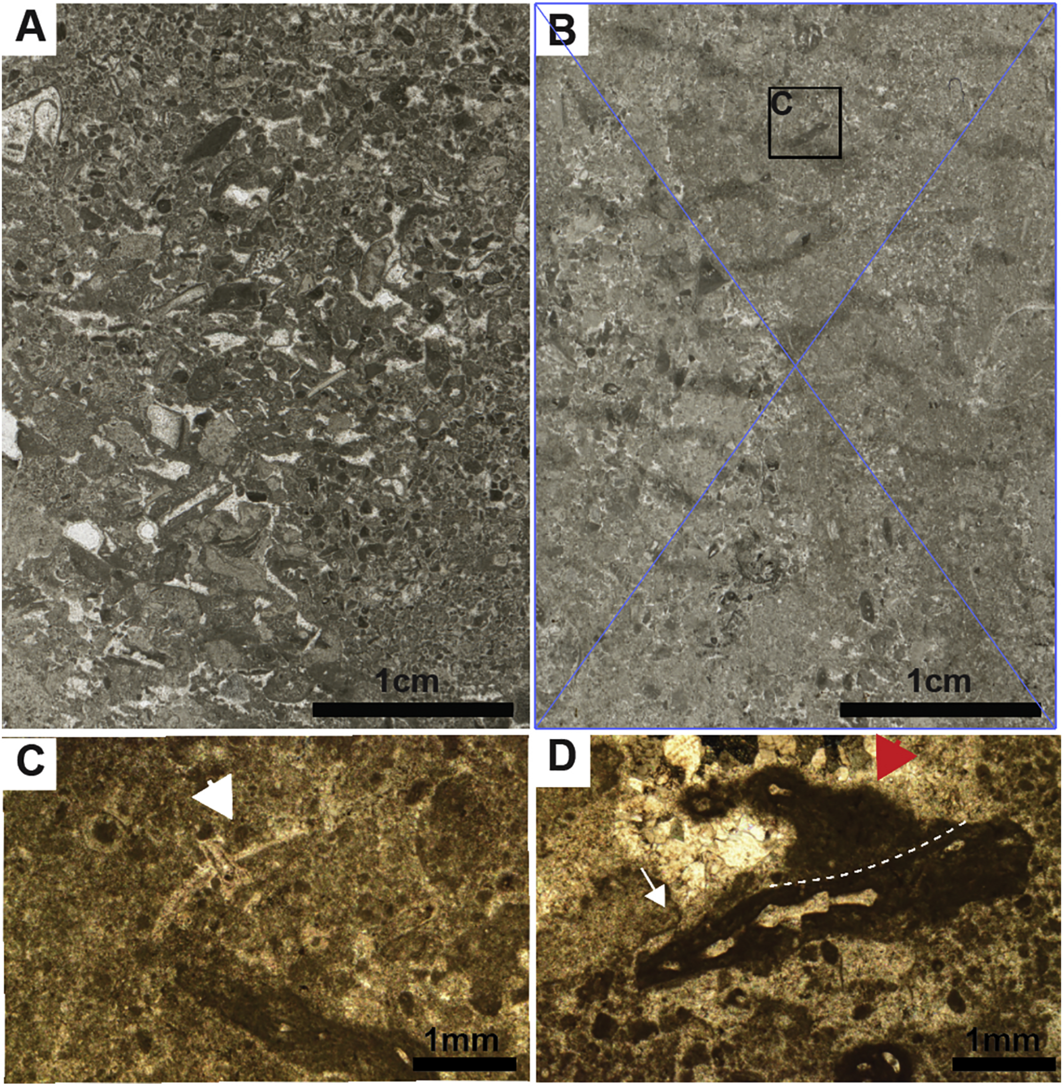

Figure 9

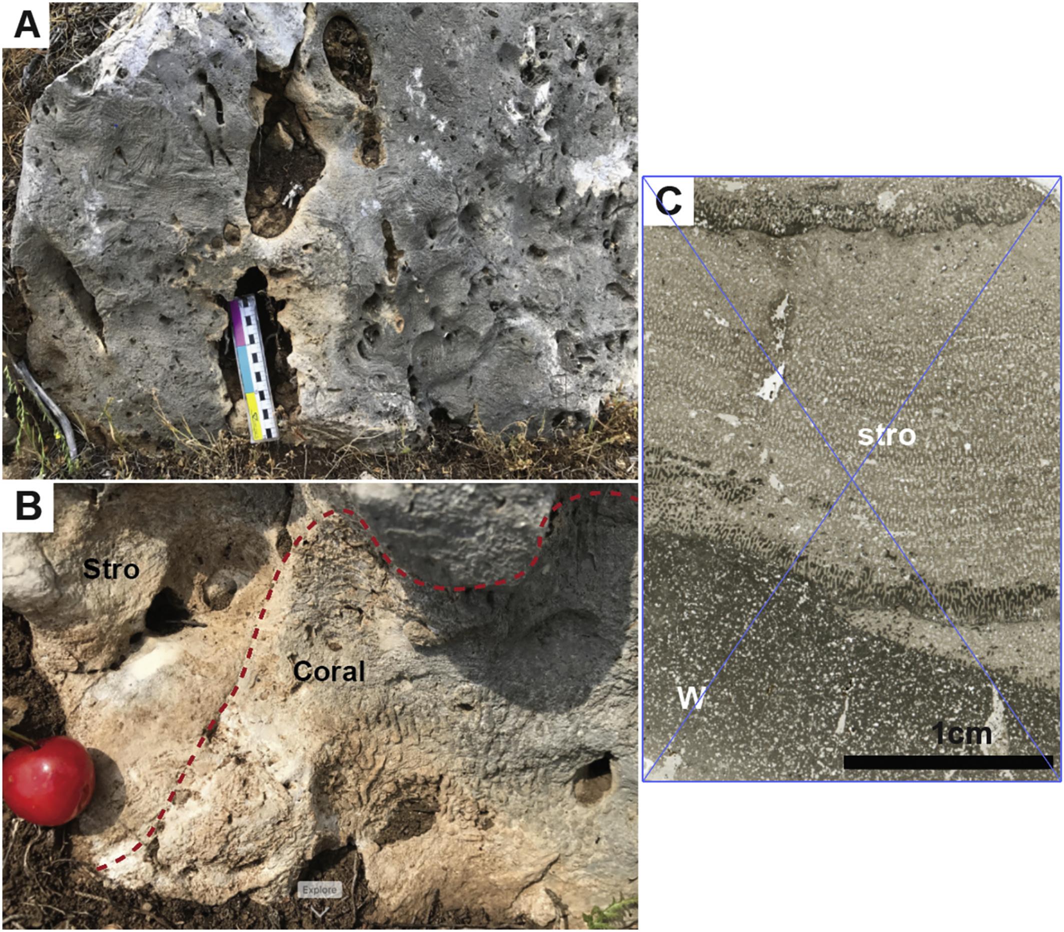

Figure 10

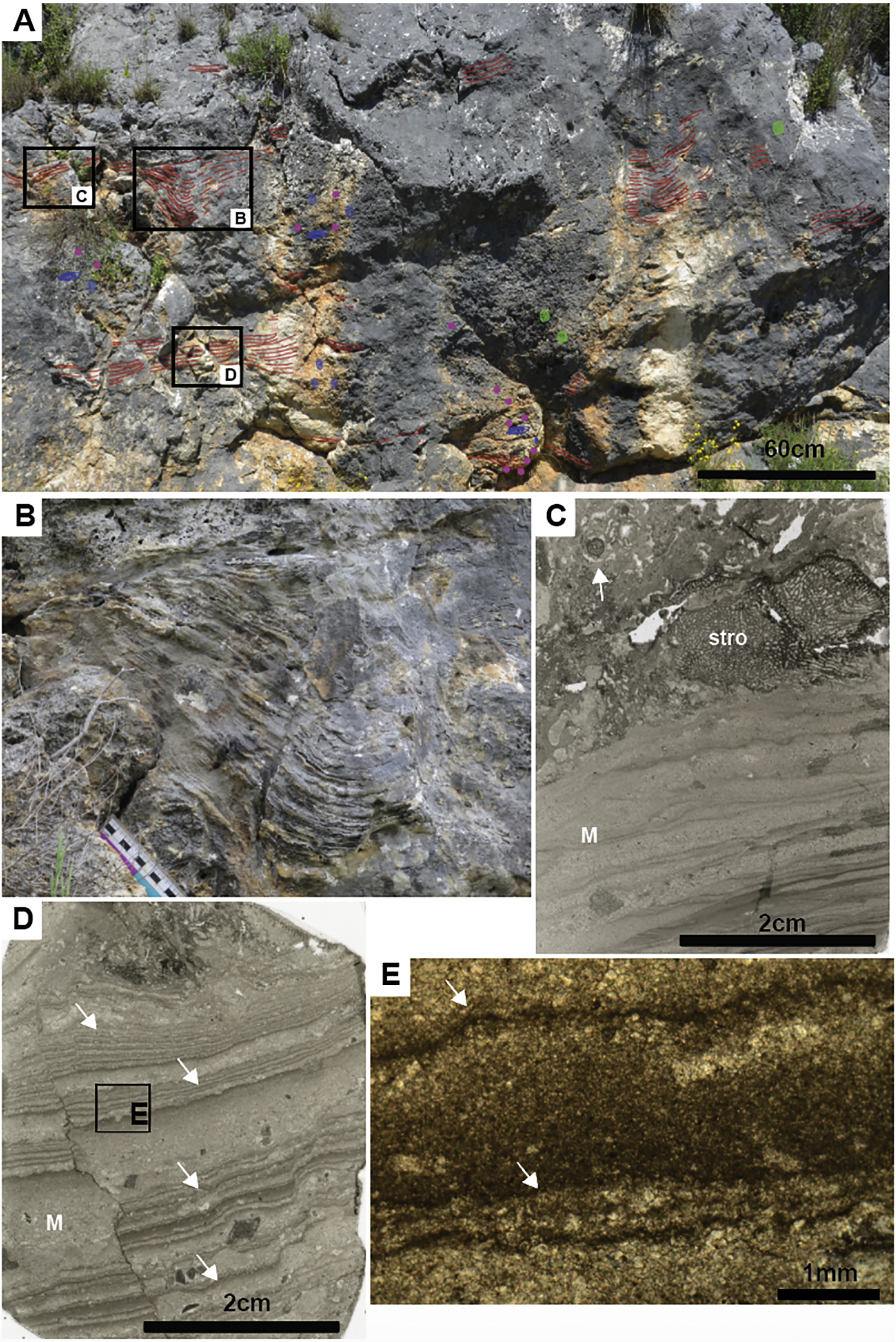

Figure 11

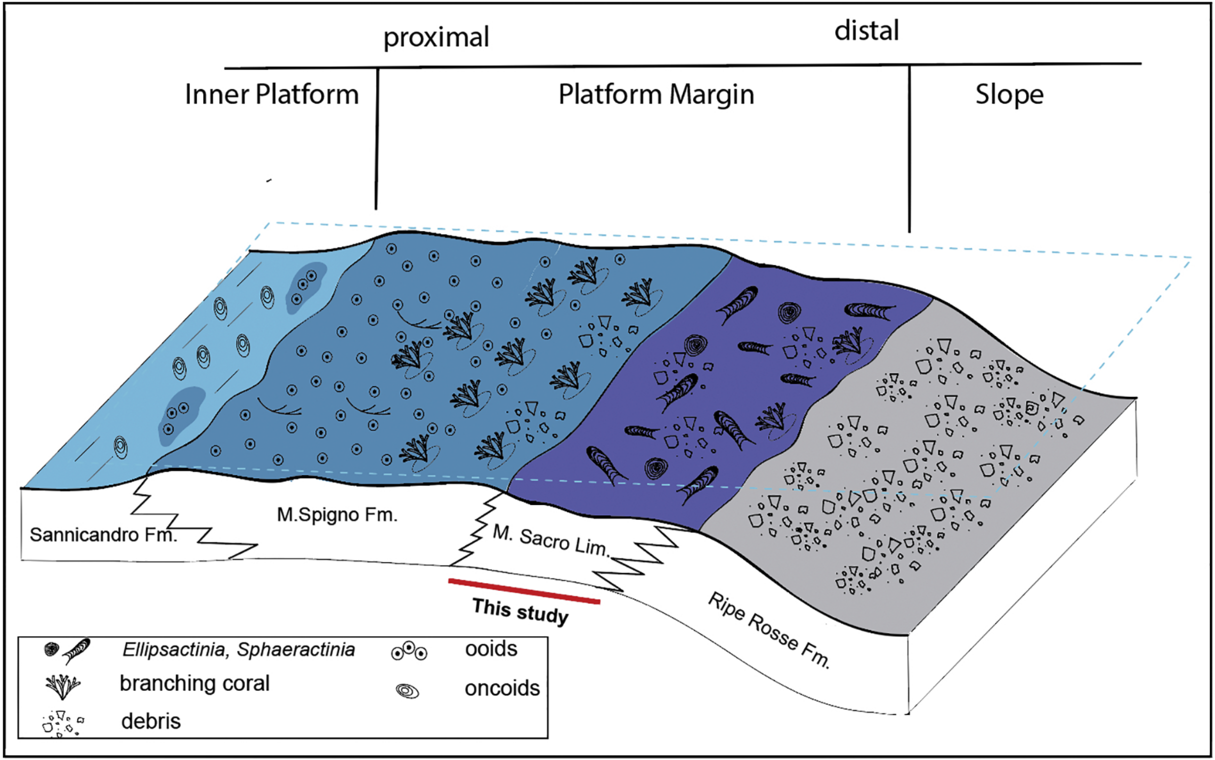
proximal
distal
Inner Platform
Platform Margin
Slope
Sannicandro Fm.
M.Spigno Fm.
M. Sacro Lim.
Ripe Rosse Fm.
This study
Ellipsactinia, Sphaeractinia
branching coral
debris
ooids
oncoids

Figure 12

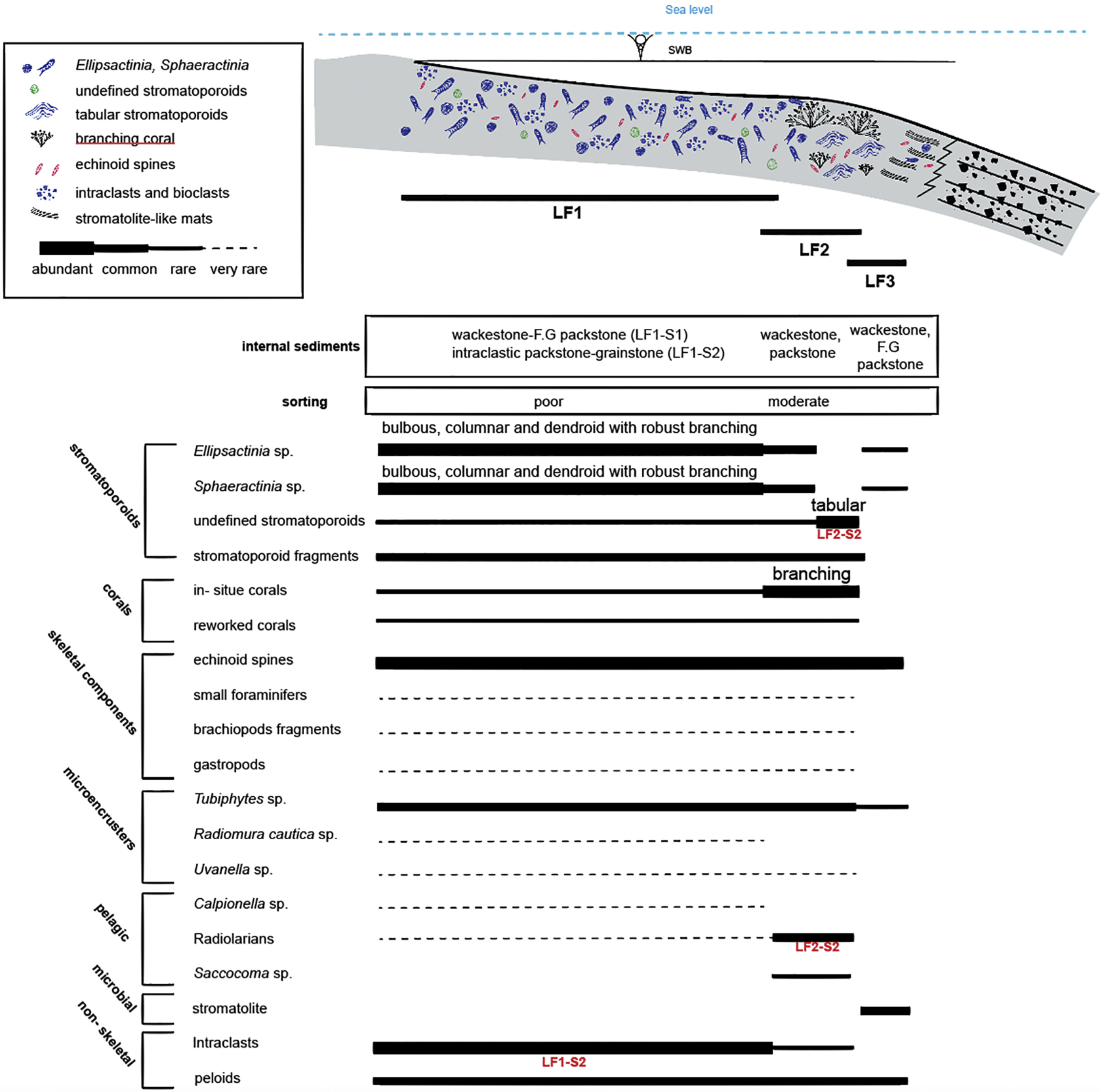
Sea level
SWB
Ellipsactinia, Sphaeractinia
undefined stromatoporoids
tabular stromatoporoids
branching coral
echinoid spines
intraclasts and bioclasts
stromatolite-like mats
abundant common rare very rare
LF1
LF2
LF3
internal sediments
wackestone-F.G packstone (LF1-S1)
intraclastic packstone-grainstone (LF1-S2)
wackestone, packstone
wackestone, F.G packstone
sorting
poor
moderate
stromatoporoids
bulbous, columnar and dendroid with robust branching
Ellipsactinia sp.
bulbous, columnar and dendroid with robust branching
Sphaeractinia sp.
tabular
undefined stromatoporoids
LF2-S2
stromatoporoid fragments
corals
branching
in- situe corals
reworked corals
skeletal components
echinoid spines
small foraminifers
brachiopods fragments
gastropods
microencrusters
Tubiphytes sp.
Radiomura cautica sp.
Uvanella sp.
pelagic
Calpionella sp.
Radiolarians
LF2-S2
Saccocoma sp.
microbial
stromatolite
non- skeletal
Intraclasts
LF1-S2
peloids

Figure 13

	Apulia Carbonate Platform (Intra- Tethys)	Northern Tethys		
Environment	pure carbonate	pure carbonate	mixed carbonate- siliciclastic	clay rich
Biota	mixed phototrophic- heterotrophic dominated	phototrophic dominated	mixed phototrophic- heterotrophic dominated	heterotrophic dominated
Nutrient availability	moderate oligotroph to mild mesotroph	nutrient poor oligotroph	moderate nutrient availability mesotroph	high nutrien level eutrophic
Light	moderate light (mesophotic)	clear water- good light (euphotic)	moderate light (mesophotic)	limited light (oligophotic)
Energy	High energy events	high energy	low energy affected by episodic storms	low energy
Platform type	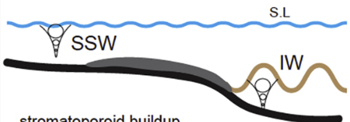	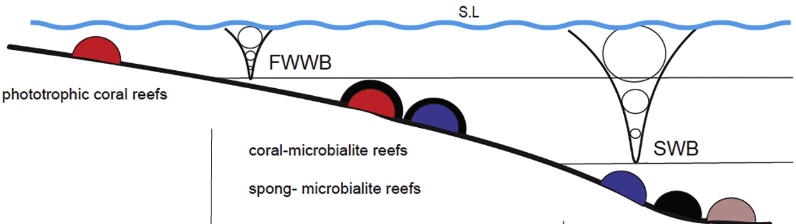		
Reef type	stromatoporoid buildup stromatoporoid-coral buildup	phototrophic coral reefs	coral-microbialite reefs spong- microbialite reefs	silicious sponge mound pure microbialite reefs microsolenid biostromes reefs
Microencrusters	*Tubiphytes morronensis*	*Lithocodium- Bacinella*	*Terebella* association	*Terebella lapilloides, Tubiphytes morronensis*

Figure 14

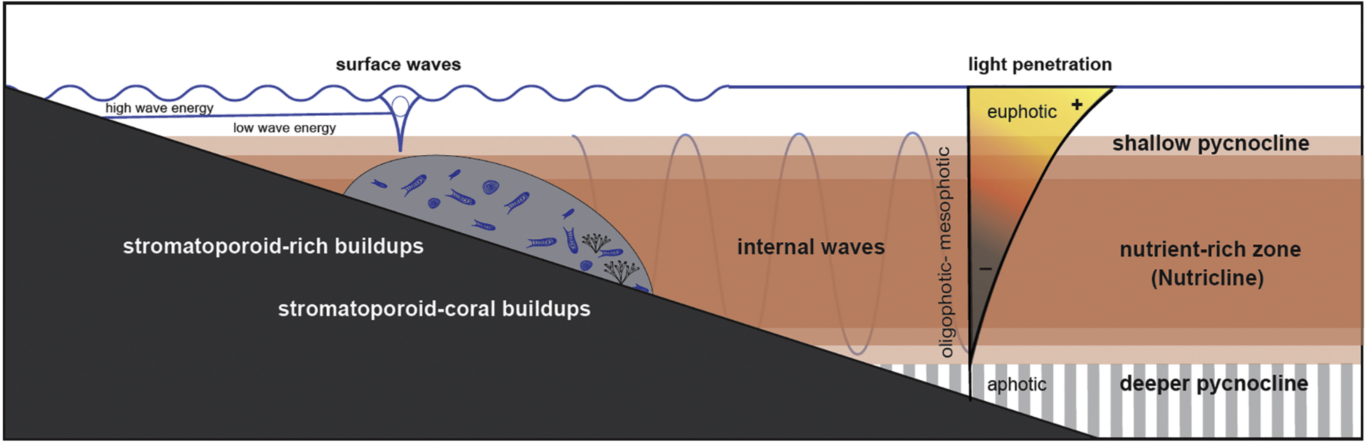
surface waves
light penetration
high wave energy
low wave energy
euphotic
+
shallow pycnocline
oligophotic- mesophotic
stromatoporoid-rich buildups
internal waves
nutrient-rich zone
(Nutricline)
–
stromatoporoid-coral buildups
aphotic
deeper pycnocline

Figure 15

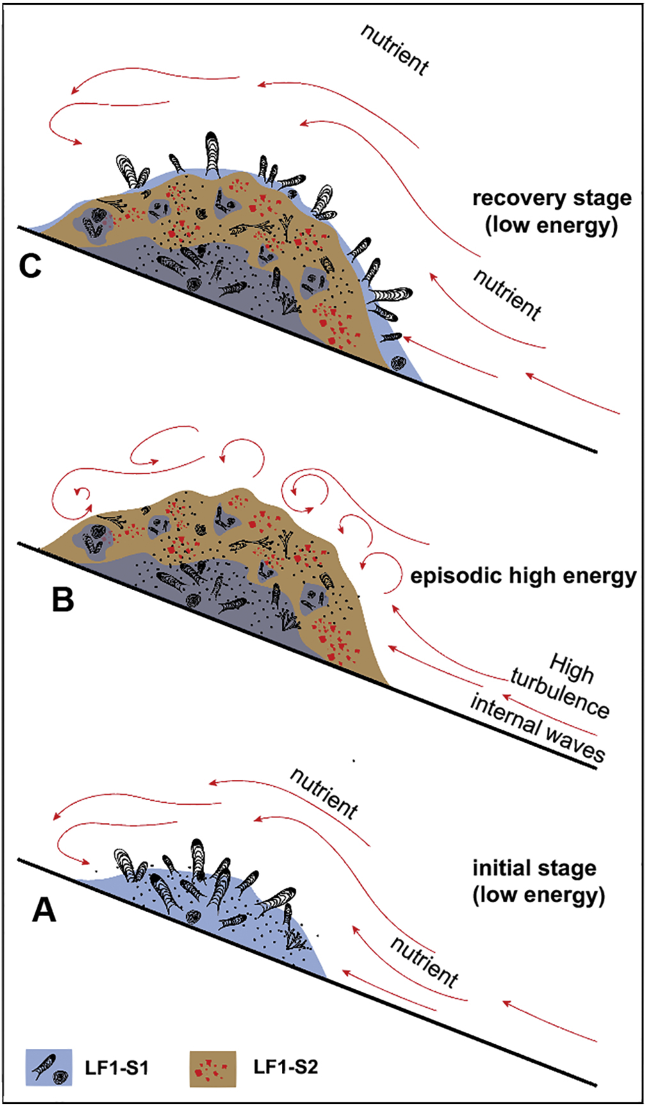
nutrient
recovery stage
(low energy)
C
nutrient
episodic high energy
B
High
turbulence
internal waves
nutrient
initial stage
(low energy)
A
nutrient
LF1-S1
LF1-S2

Figure 16